DR. LIXUE CHEN (Orcid ID : 0000-0001-8213-8828)

Article type : Original Article

Upregulation of astrocyte excitatory amino acid transporter 2 alleviates central sensitization in a rat model of chronic migraine

Xue Zhou [a], Jie Liang [a], Jiang Wang [a], Zhaoyang Fei [a], Guangcheng Qin [a], Dunke Zhang[a], Jiying Zhou [b], Lixue Chen [a*]

[a*]Laboratory Research Center, The First Affiliated Hospital of Chongqing Medical University, Chongqing, China

[b] Department of Neurology, The First Affiliated Hospital of Chongqing Medical University, Chongqing, China

***Corresponding author**:

Lixue Chen, Laboratory Research Center, The First Affiliated Hospital of Chongqing

Medical University, 1st You Yi Road, Yu Zhong District, Chongqing, China, 400016

Email: chenlixue@hospital.cqmu.edu.cn

Telephone number: +86 23 89012105

Fax: +86-023-8911487

Abbreviations

Cef, Ceftriaxone; CGRP, calcitonin gene-related peptide; CM, chronic migraine; CNS, central nervous system;

CREB, cAMP response element binding protein; CREB-pSer, serine-phosphorylated; EAAT2, excitatory amino acid transporter 2; GFAP, glial fibrillary acidic protein; HD, high dose; HPLC, high-performance liquid chromatography; LD, low dose; NMDA, N-methyl-D-aspartate; NR2B-pTyr, tyrosine-phosphorylated NR2B; PSD, postsynaptic density; PSD95, postsynaptic density 95; SP, substance P; Syt-1: synaptotagmin1; TEM, transmission electron microscope; TGVS, trigeminovascular system; TG, trigeminal ganglion; TNC, trigeminal nucleus caudalis

Abstract

Central sensitization is the potential pathogenesis of chronic migraine (CM) and is related to persistent neuronal hyperexcitability. Dysfunction of excitatory amino acid transporter 2 (EAAT2) leads to the accumulation of glutamate in the synaptic cleft, which may contribute to central sensitization by overactivating glutamate N-methyl-D-aspartate (NMDA) receptors and enhancing synaptic plasticity. However, the therapeutic potential of CM by targeting glutamate clearance remains largely unexplored. The purpose of this study was to investigate the role of EAAT2 in CM central sensitization and explore the effect of EAAT2 expression enhancer LDN-212320 in CM rats. The glutamate concentration was measured by high-performance liquid chromatography (HPLC) in a rat model of CM. Then, q-PCR and Western blots were performed to detect EAAT2 expression, and the immunoreactivity of astrocytes was detected by immunofluorescence staining. To understand the effect of EAAT2 on central sensitization of CM, mechanical and thermal hyperalgesia and central sensitization-associated proteins were examined after administration of LDN-212320. In addition, the expression of synaptic-associated proteins was examined and Golgi-Cox staining was used to observe the dendritic spine density of TNC neurons. Also, the synaptic ultrastructure was observed by transmission electron microscope (TEM) to explore the changes of synaptic plasticity. In our study, elevated glutamate concentration and decreased EAAT2 expression were found in the TNC of CM rats, administration of LDN-212320 greatly upregulated the protein expression of EAAT2, alleviated hyperalgesia, decreased the concentration of glutamate and the activation of astrocytes. Furthermore, reductions in calcitonin gene-related peptide (CGRP), substance P(SP), and phosphorylated NR2B were examined after administration of LDN-212320. Moreover, evaluation of the synaptic structure, synaptic plasticity- and central sensitization-related proteins indicated that EAAT2 might participate in the CM central sensitization process by regulating synaptic plasticity. Taken together, upregulation of EAAT2 expression has a protective effect in CM rats, and LDN-212320 may have clinical therapeutic potential.

Keywords:

Chronic migraine Glutamate Glutamate transporters Synaptic plasticity Central sensitization Astrocyte

Introduction

Migraine is a common clinical disorder of the central nervous system (CNS) that afflicts up to 15% of the world's population (Lipton *et al.* 2007), and approximately 2.5% of people with episodic migraine develop chronic migraine (CM) each year. CM patients' life and work are both severely affected during headache attacks. The molecular mechanism of CM is not fully understood, effective drugs and treatments are currently lacking, and more than half of the CM patients report dissatisfaction with their treatments (Tfelt-Hansen & Olesen 2012). Therefore, there is an urgent need for effective drugs and treatment strategies.

Central sensitization is thought to be the underlying mechanism of CM, which suggests that peripheral nociceptive stimulation leads to an increase in the excitability and synaptic efficacy of the central neurons in the nociceptive pathway of the trigeminal nerve, predominantly the trigeminal nucleus caudalis (TNC) (Bernstein & Burstein 2012; Mathew 2011). The induction and maintenance of central sensitization depends on the activation of glutamate N-methyl-D-aspartate (NMDA) receptors, revealing the key participation of glutamate and its receptors (Latremoliere & Woolf 2009; Woolf & Thompson 1991).

Glutamate, as the most important and major excitatory neurotransmitter in the CNS, is essential for the development of the nervous system and the maintenance of synaptic plasticity (Willard & Koochekpour 2013; Gegelashvili & Bjerrum 2014). Under disease conditions, abnormal release of glutamate and/or dysfunction of glutamate clearance result in elevated extracellular glutamate concentrations. This causes excessive stimulation of glutamate NMDA receptors, leading to enhancement of synaptic plasticity, and an abnormal excitability of neurons, thus inducing central sensitization (Latremoliere & Woolf 2009).

NMDA receptor blockade has been extensively studied to attenuate excitatory synaptic transmission in a variety of neurological diseases. In our previous study, inhibition of phosphorylated NR2B (the most important tyrosine phosphorylation protein of NMDA receptors) alleviated allodynia in CM rats (Wang *et al.* 2018). However, neuroprotective effects were obtained in animal experiments using glutamate receptor antagonists, their clinical application maybe limited by their neurotoxicity and the considerable mental side effects(Boyko *et al.* 2014; Li *et al.*

2002). Therefore, targeting the glutamate clearance to reduce the NMDA receptors activation may be a more effective way to lower the excitability of neurons.

Excitatory amino acid transporter 2 (EAAT2), as a glutamate scavenger, is responsible for the majority of glutamate uptake (90%) and predominantly expressed on astrocytes (Rao *et al.* 2015; Danbolt 2001; Gegelashvili & Bjerrum 2019). Pronounced changes in the expression and function of EAAT2 may occur after damage to the CNS. Downregulation of the expression of EAAT2 and dysfunction of the glutamate uptake system would lead to sustained accumulation of extracellular glutamate and be the main cause of excitotoxicity. Recovery of EAAT2 expression levels and function have a good clearance of extracellular glutamate and thus prevent the excitotoxicity of neurons. LDN-212320 is a new generation of EAAT2 expression enhancer and has a potent ability to increase EAAT2 expression through translational activation, which shows a prominent protective effect in animal models of ALS and epilepsy (Takahashi *et al.* 2015b; Kong *et al.* 2014).

However, since neurons have been the focus of CM treatments, few studies have been conducted to explore the role of astrocytes in the central sensitization mechanism of CM. Whether astrocyte EAAT2 is a potential therapeutic target for CM and the therapeutic potential of LDN-212320 stays unclear. In this study, we investigated the role of astrocyte EAAT2 in the central sensitization mechanism of CM, and assessed the therapeutic effect of LDN-212320 on CM rats. The expression levels of EAAT2 in TNC were decreased in a rat model of CM, and upregulation of EAAT2 alleviated central sensitization by reducing the synaptic plasticity in CM rats. In addition, LDN-212320 showed a good effect on upregulating the expression of EAAT2 and analgesia in CM rats. Our study provides the first experimental evidence that EAAT2 is a potential therapeutic target of CM and LDN-212320 has a neuroprotection effect in CM animal studies.

Experimental procedures

Animals

A total of 205 healthy adult male Sprague–Dawley rats (250–300 g, RRID: 2012–0001) born and raised in the Experimental Animal Center of Chongqing Medical University (Chongqing, China) were used for this study. Rats were housed in plastic cages (20 cm in height, 30 cm in width and 40 cm in length) with 5 rats per cage and

maintained in a standard experimental environment with a 12:12 light and dark cycle at room temperature of 22 ± 1 °C where they were free to access water and food. Before the experiment, rats were acclimatized for one week and assigned to each experimental group after a simple randomization. The process of the simple randomization in this study was as follows: (1) First, male SD rats of 250~300g were numbered, then entering the numbers into the Excel form. (2) Next, randomized numbers were created by using the "rand" function of the Excel software and then were sorted in ascending order. (3) At last, according to the sorting, every 6~10 numbers were divided into different groups. The time-line and experimental procedures of this study are illustrated in Fig. 1. The experiments were carried out between 9:00 and 17:00 h. During the trials, the experimenter was blinded to animals' group assignment, and no statistical method was used to determine the sample size of this study. The study was carried out after being approved by the Ethics Committee of the Department of Medical Research at the First Affiliated Hospital of Chongqing Medical University and the ethical approval reference number is 20187401. All procedures followed the National Institutes of Health Guide for the Care and Use of Laboratory Animals. The study was not pre-registered.

Surgery

Rats were fasted for 12 hours before craniotomy and cannula fixation to prevent abdominal dilation. Rats were anesthetized with chloral hydrate combined with analgesics. Isoflurane was not used for anesthesia due to the lack of ventilator equipment in our laboratory, and compared with pentobarbital sodium, the combination use of chloral hydrate and analgesics can achieve a good anesthetic effect during the surgery and reduce the mortality of rats caused by anesthesia. Therefore, the combination use of chloral hydrate and analgesics was selected in our study for animal anesthesia. Rats were first anesthetized with 10% chloral hydrate (4 ml/kg, intraperitoneal), then 0.01 mg/kg buprenorphine was injected subcutaneously for analgesia. In addition, 1 ml of bupivacaine (5 mg/1 ml) was applied as a local preventive anesthetic under the surgical area of the skin as described in our previously studies(Liu *et al.* 2018; He *et al.* 2019), and placed in a stereotactic instrument (ST-51603; Stoelting Co., Chicago, IL, USA). The surgical area was first disinfected with iodide, and an incision was made on the midline of each rat's head by using a surgical blade to completely expose the skull. Then, a 1-mm diameter craniotomy (+1.5 mm from bregma, +1.5 mm lateral) was performed carefully using a burr drill, and attention was taken not to damage the dura mater. Rat with damaged dura mater will be excluded from the experiment. A total of 205 rats underwent surgery and 9 rats were excluded due to the dural damage during the surgery (2 in CM group, 1 in CM+dimethyl sulfoxide (DMSO) group, 3 in

CM+LDN-212320 low dose (LD) group, 2 in sham+LDN-212320 LD group and 1 in sham group were excluded). Subsequently, the cannula was fixed to the skull using dental fixation acrylic, and then inflammatory soup or phosphate buffered saline (PBS) could be delivered to the dura through the cannula. A matched occlusion cap was used to seal the cannula. After the skin was sutured with 4-0 nylon, the rats were placed on a thermostat until they awoke from anesthesia (about 1-2 hours later). The last step, before the follow-up experiments, was to place the rats back to in their clean cages individually for one week and restoring them to pre-operative activity levels. The wound was disinfected daily after the surgery, rats with no abscess in the surgical areas and the thermal and mechanical pain thresholds returning to the pre-operative levels 7 days after the operation were selected for the next experiments (2 in sham group, 1 in CM group, 1 in CM+ LDN-212320 LD were excluded due to the infection at the surgical sites; 1 in CM+Ceftriaxone (Cef) LD group, 1 in CM+DMSO group were excluded because the thermal and mechanical thresholds did not return to the pre-operative levels after seven days). The excluded rats were replaced in the group and experimental stage in which they were excluded. To minimize animal suffering, the depth of the anesthesia was carefully monitored and the analgesic drugs of buprenorphine and bupivacaine were used to minimize the pain during the experiments.

Repeated dural infusions

Rats were placed in individual transparent glass cages and allocated to either the CM group or the sham group using the simple randomization method described above. Rats in the CM group were stimulated with inflammatory soup for 7 days;inflammatory soup was composed of 1 mM serotonin (Sigma-Aldrich, Cat.No. H7752, (year 2018)), 1 mM bradykinin (Sigma-Aldrich, Cat.No. B3259, (year 2018)), 1 mM histamine (Sigma-Aldrich, Cat.No. H7375, (year 2018)) and 0.1 mM prostaglandin E2 (Sigma-Aldrich, Cat.No. P5640, (year 2018)), which was dissolved in PBS (pH 7.4). The sham group received PBS of the same volume as the CM group for 7 consecutive days. 2 μl of inflammatory soup or PBS was stably delivered to the dura mater in 5 minutes by using a microinfusion pump through the cannula, and rats were free to move during the infusion.

Behavioral pain tests

Mechanical pain thresholds and the thermal pain thresholds were measured as a baseline prior to the first inflammatory soup or PBS infusion, and the tests were performed 24 hours after each dural infusion and before the next dural stimulation.

Mechanical allodynia

To assess mechanical allodynia, withdrawal thresholds of the periorbital and hind paw in rats were measured using the Von Frey test as previously described (Zhou *et al.* 2019). Rats were placed in wire mesh cages (16 cm in height, 14 cm in width and 27 cm in length) individually for 30 minutes of acclimatization, and then stimulated with the pressure probe tip of the electronic von Frey apparatus (Electrovonfrey, no. 2450, IITC, Inc., Woodland Hills, CA, USA) at the periorbital and hind paw areas. The generated force values of the device ranged from 0 to 900 g, and stimulations gradually increased until positive reactions of rats occurred, such as rapid claw lifting and head retraction. Each rat was tested at least three times per site with an interval of one minute of each stimulation.

Thermal allodynia

Thermal allodynia after repeated dura inflammatory soup infusions was evaluated by a plantar test instrument (model PL-200, IITC, Taimeng, Chengdu, China) based on Hargreaves' method (Hargreaves *et al.* 1988). Briefly, after 30 minutes of acclimation in a smooth, glass-floored transparent cage (15 cm in height, 20 cm in width and 20 cm in length), infrared radiation (intensity: 20) was applied to the center of each rat's hind paw, and withdrawal latency was recorded automatically when the hind paw moved. Stimulation was stopped after 20 seconds to prevent tissue damage, and each rat was recorded three times to calculate the average latency.

Drug administration

To understand the role of EAAT2 in CM rats, animals were treated with EAAT2 expression enhancers LDN-212320 (MedChemExpress / MCE, Cat.No. HY-12741 (year 2018), American) and Cef (Selleck, Cat.No. S4158, (year 2018), China) (Fontana 2015). Rats were randomizedinto the following groups using a simple randomization method as described above: (1) sham group, (2) CM group, (3) CM+DMSO group, (4) CM+LDN-212320 LD group (5 μg), (5) CM+LDN-212320 high dose (HD) group (20 μg), (6) CM +Cef LD group (50 μg), (7) CM+Cef HD group (200 μg), (8) sham+LDN-212320 HD group (20 μg). The doses of LDN-212320 and Cef were based on the previous studies (Kong *et al.* 2014; Chen *et al.* 2016). Rats were anesthetized with 10% chloral hydrate (4 ml/kg, intraperitoneal) and subcutaneously injected with 0.01 mg/kg buprenorphine the day after the 7th inflammatory soup infusion and injected with the designated treatment solution (5 μl) in the lateral ventricle (− 1.0 mm rear from the bregma, + 1.5 mm lateral to the bregma, 4.0 mm from the skull plane). An equal volume of DMSO was used as the corresponding vehicle

control.

High-performance liquid chromatography (HPLC)

The total glutamate concentration in the TNC was measured by HPLC. After anesthesia with 10% chloral hydrate (4 ml/kg, intraperitoneal) and subcutaneous injected with 0.01 mg/kg buprenorphine, rats were killed through rapid decapitation. Subsequently, the TNC areas were separated in a glass dish placed on ice. To remove the surface blood, tissues were washed in PBS for 2 to 3 seconds, then the PBS solution attached to the tissues was absorbed with the filter paper. After the tissues were precisely weighed, was added the internal standard solution at weight 1:1 (mg : μl) and then fully homogenized the tissues, the internal standard solution was BABA (3-aminobutyric acid) solution with a concentration of 600 μg/mL prepared with the ultra-pure water. In accordance with the weight ratio 1:5 (mg : μl), acetonitrile was added to precipitate the proteins, and then centrifuged at 4 °C (12000 xg, 10 min). The supernatants were diluted 10 times to obtain the sample to be tested, and the glutamate concentration was determined by HPLC.

Quantitative real-time polymerase chain reaction (q-PCR)

Total RNA was extracted from TNC fragments using the RNAiso Plus reagent (TaKaRa, Cat.No. 9108, (year 2018), Dalian, China) according to the manufacturer's instructions. Then, the RNA yield and purity were assessed using NanoDrop (Thermo, USA), and cDNA was synthesized using PrimeScript TM RT kit (TaKaRa,Cat.No. 5005, (year 2018)). To quantify the expression of EAAT2, q-PCR was performed on a CFX96 Touch thermocycler (Bio-Rad) using SYBR® Premix Ex Taq™ II (Takara, Cat.No. RR820A, (year 2018)). Primer sequences for EAAT2 and GADPH (Sangon Biotech, Shanghai, China) were used as follows:

EAAT2 (Forward Primer): 5'-CTTTGCCTGTCACCTTCCGT-3', ETTA2 (Reverse Primer): 5'-GGGCTGTACCATCCATGTTAA-3';

GAPDH(Forward Primer): 5'-ATGACTCTACCCACGGCAAGC-3', GAPDH(Reverse Primer): 5'-GGATGCAGGGATGATGTTCT-3'.

PCR amplification was carried out at 95 ° C for 30 seconds, followed by 45 cycles of 95 °C for 5 s and 55 °C for 30 s. GAPDH was used as an endogenous control to normalize differences. All fluorescence data were processed by a PCR post-data analysis software program. The differences of gene expression were analyzed with the $2^{-\Delta\Delta CT}$ method.

Western blot analysis

The fresh TNC tissues were homogenized in RIPA lysis buffer (Beyotime, Cat.No. P0013B (year 2018), China) containing proteinase inhibitors (Beyotime, Cat.No. P1030 (year 2018), China) and phosphatase inhibitors (Beyotime, Cat.No. AR1183 (year 2018), China) and homogenized at 4 ℃ for 2 hours. Then, the BCA protein assay kit (Beyotime, Cat.No. P0012S, year 2018) was used to detect protein concentrations. An equal amount of protein (40 μg) was loaded on 10% SDS-PAGE gels (Beyotime, China) for electrophoresis and transferred to a polyvinylidene difluoride (PVDF) membrane (Millipore, USA). The membranes were blocked with 5% skim milk for two hours at room temperature and incubated overnight at 4 °C with the following primary antibodies: anti-EAAT2 (1:1000, RRID: AB_2190743, Cell Signaling Technology, USA), anti-CGRP (1:2000, RRID: AB_725807, Abcam, UK), anti-CREB (1:500, RRID: AB_2567681, Wanleibio, China), anti-pCREB-S133 (1:3000, RRID: Addgene_15222, Abcam, UK), anti-CREB-S129 (1:1000, RRID: AB_895223, Signalway, USA), anti-c-Fos (1:3000, RRID: AB_530851, Novus Biologicals, USA), anti-NR2B (1:1000, RRID: AB_10667005, Proteintech), anti-pNR2B-Y1472 (1:1000, RRID: AB_11074382, Bioss, China), anti-pNR2B-Y1474 (1:500, RRID: AB_304114, Abcam), anti-PSD95 (1:1000, RRID: AB_298846, Abcam), anti-synaptophysin (1:5000, RRID: AB_765072, Abcam), anti-synaptotagmin-1 (1:500, RRID: AB_778216, Abcam), anti-GAPDH (1:5000, RRID: AB_2617427, Abways Technology, China) and anti-β-actin (1:5000, RRID: AB_2750915, Proteintech). The next day, membranes were washed with Tris-buffered saline Tween 20 (TBST) buffer three times and then incubated with Horseradish peroxidase-conjugated anti-rabbit (1:5000, RRID: AB_10856483, Bioss) or anti-mouse secondary antibodies (1:5000, RRID: AB_10858521, Bioss) for 1 h at room temperature. All blots were detected using a BeyoECL Plus kit (Beyotime). The intensity of the scanned images was analyzed using the imaging system (Fusion, Germany).

Immunofluorescence staining (IF)

After anesthesia with 10% chloral hydrate (4 ml/kg, intraperitoneal) and subcutaneous injection with 0.01 mg/kg buprenorphine, rats were perfused intracardially with 0.9% saline and then with 4% paraformaldehyde in 0.1% PBS (pH 7.4). The areas from the medulla oblongata to the first cervical cord were fixed overnight in 4% paraformaldehyde and successively immersed in a gradually increased concentration of sucrose solution (20% to 30%) until the tissues sank to the bottom. The coronal sections of the TNC were cut into 10 μm sections using a low temperature thermostat (Leica, Japan). For immunofluorescence staining, sections were first washed three times with

PBS and then incubated with 0.3% Triton X-100 (Beyotime) for 10 minutes, followed by blocking with 10% normal goat serum for 30 minutes at 37 °C. Then, sections were incubated overnight with the following primary antibodies at 4 °C: anti-EAAT2 (1:100, RRID: AB_2190743, Cell Signaling Technology), anti-CGRP (1:50, RRID: AB_629364, Santa Cruz Biotechnology, USA), anti-GFAP (1:100, RRID: AB_1124889, Santa Cruz Biotechnology), anti-substance P (SP) (1:50, RRID: AB_297089, Abcam). On the next day, the sections were rinsed three times with PBS and incubated with the corresponding secondary antibodies for 90 minutes at 37 °C: Cy3-conjugated goat anti-mouse IgG (1:200, Beyotime, Cat.No. A0521 (year 2018)), Alexa Fluor 488-conjugated goat anti-mouse IgG (1:200, Beyotime, Cat.No. A0428 (year 2018)) and Alexa Fluor 488-conjugated goat anti-rabbit IgG (1:200, Beyotime, Cat.No. A0423 (year 2018)). Then, sections were washed in PBS three times and incubated with 4′,6-diamidino-2-phenylindole (DAPI) (Beyotime) for nuclear staining at 37 °C for 10 minutes. Negative control sections were incubated with PBS, and micrographs were analyzed using a fluorescence confocal microscope (ZEISS, Germany). To determine the immunoreactivity of EAAT2, GFAP, CGRP, SP in the TNC, five slices for each rat were arbitrarily selected (n = 6 rats per group and 5 images per animal).

Immunofluorescence imaging data analysis

First, sections were observed under the confocal laser scanning fluorescence microscope to find the TNC regions. Exemplary shown in Fig. 2, the white dotted frame represents the TNC regions. Five TNC sections were arbitrarily selected from each rat;6 rats were analyzed in each group. Image-pro Plus 6.2 software (Bethesda, MD, USA) was used to analyze the images. The white solid line rectangular box as shown in Fig. 2 of TNC areas were selected for the analysis of astrocytes, and the ratio of the number of astrocytes (labeled by GFAP) to the number of total cells (labeled by DAPI) was analyzed under a 20x objective. The mean optical density (OD) were used to analyze the fluorescence intensity of CGRP and SP in the TNC at x10 magnification. During the whole process of taking and analyzing the pictures, the experimenters were only shown the encoding numbers and thus blinded to the experimental group allocation of the respective sample. After the pictures had been taken for all the samples and the analysis statistical analysis completed, the group information and the corresponding coding numbers were revealed to experimenters by the person who had encoded the samples.

Transmission electron microscopy (TEM)

For TEM, rats were anesthetized with 10% chloral hydrate (4 ml/kg, intraperitoneal) and subcutaneously injected with

0.01 mg/kg buprenorphine, then perfused intracardially with 2.5% glutaraldehyde and the TNC tissues were dissected and separated rapidly and soaked overnight in 4% glutaraldehyde at 4 °C. Next, the TNC tissues were cut into 3 1-mm pieces with a sharp blade and sent to Chongqing Medical University for subsequent fixation, embedding, slicing and staining. Since the glutamatergic synapses are primarily asymmetric synapses (Izzo & Bolam 1988), based on three classical criteria for determining the excitatory asymmetric synapses (Guldner & Ingham 1980; Kobayashi *et al.* 2014): 1) clear circular vesicles, 2) dense postsynaptic density, 3) wide synaptic gap, the asymmetric synapses were selected for analysis in this study. Ten micrographs were arbitrarily taken from each rat using an EM-1400 PLUS transmission electron microscope (TEM) and the image analysis was performed using Image-pro Plus 6.2. The thickness of the PSD and the length of the synaptic activity zone were measured according to the method of Güldner and Ingham (Guldner & Ingham 1980), the width of the synaptic cleft was measured by the multipoint averaging method and the curvature of the synaptic interface was measured base on the method of Jones and Devon (Jones & Devon 1978). During the whole process of taking and analyzing the pictures, the experimenters were blinded to the experimental groups (only shown the encoding numbers). After pictures had been taken from all the samples and the statistical analysis completed, the grouping information and the corresponding coding numbers would be revealed to experimenters by the person responsible for encoding the samples (n = 6 rats per group, 10 images per animal).

Golgi-cox staining

The fresh samples of TNC regions were isolated in a glass dish placed on ice and washed with double distilled water for 2-3 seconds to remove the blood from the surface. A Golgi Rapid Staining Kit (FD Neuro Technologies) was used for subsequent tissue preparation and staining procedures, and the entire procedure was performed in strict accordance with the manufacturer's user manual and material safety data sheet. The extracted TNC tissues were immersed in the Rapid Golgi-cox solution (solution A/B) prepared one day in advance (the solution was changed after 24 hours) for 14 days and then transferred to the Solution C (the solution was changed after 24 hours) for three days. The whole process was carried out at room temperature and protected from light. A series of 150-micron coronal sections were cut with a vibratome (Leica VT 1200S, Japan) to ensure inclusion of the entire (non-transected) neural arbor, and the sections were then applied to gelatin-coated slides. The slides were further processed in accordance with the manufacturer's instructions and finally covered with Permount™ Mounting Medium (Fisher Scientific Co, Waltham, MA, USA). The excitatory pyramidal neurons in the TNC regions were selected for dendritic spines analysis. After

Golgi-Cox staining, the pyramidal neurons can be readily identified through the following three characteristics (Perez-Cruz *et al.* 2009): (1) the characteristic triangular soma shape, (2) the apical dendrites extending toward the surface of the branches, (3) the large number of dendritic spines. Also, the selected pyramidal neurons met the following criteria: (1) the dendritic structures were in-tact, and the dendrites were clearly visible, (2) black and consistent Golgi-Cox staining was presented on the whole length of the neuron dendrites, (3) and there was enough space between each neuron to prevent interference in the analyzing process. The Image-pro Plus 6.2 software (Bethesda, MD, USA) was used to analyze the images. During the whole process of taking and analyzing the pictures, the experimenters were only shown the encoding numbers and thus blinded to the experimental groups. After pictures had been taken for all the samples and after completion of the statistical analysis, the group information and the corresponding coding numbers were revealed to the experimenter by the person responsible for encoding the samples (n = 6 rats per group, 5 images per animal).

Statistical analysis

All data are presented as the mean ± SD. SPSS 22.0 (SPSS, Inc., Chicago, IL, USA) was used for the statistical analysis. Graphs were generated using GraphPad Prism 7 (GraphPad Software, San Diego, CA, USA) and statistical analysis results were presented in box-plots (Weissgerber *et al.* 2015). Prior to statistical analysis, the Shapiro-Wilk (S-W) normality test was applied to test whether all data conformed with normality, and F test or Bartlett test, respectively, were used to test homogeneity of variance. Z-score tests were conducted using the SPSS software to identify the outliers, data with Z scores < -3 or > 3 was considered outliers, and no data was identified as outliers in this study. Behavioral data (mechanical pain thresholds and thermal pain thresholds) were evaluated using two-way analysis of variance followed by Bonferroni post-hoc test. Differences between the two groups were analyzed using an independent-sample T-test, and one-way ANOVA followed by Bonferroni post-hoc test for multiple comparisons was used for more than two groups. $P < 0.05$ was considered statistically significant.

Results

Repeated dural inflammatory soup infusions induced hyperalgesia and elevated CGRP levels

A von Frey monofilament was used to examine the changes in mechanical thresholds in the periorbital and hind paw regions of rats after repeated dural infusions of IS/PBS. The mechanical thresholds of periorbital and hind paws in the

CM group began to decrease significantly after the second IS infusion. The differences between the CM and sham groups were most obvious on the 3rd day, showing a significant downregulation of the pain thresholds in the CM group, and the pain thresholds remained decreased in the next three days after the last IS infusion (Fig. 3b, c). The thermal pain thresholds were consistent with mechanical pain thresholds (Fig. 3d). As a key neuropeptide of the trigeminal nervous system, CGRP is considered a trigger for migraine, and its expression level is closely related to the pathophysiology of CM (Edvinsson 2017). After 7 days of dural infusions, the protein expression of CGRP in the TNC of the CM group was greatly increased compared to the sham group (Fig. 3e, f).

Repeated dural inflammatory soup infusions increased the glutamate concentration and downregulated the expression of EAAT2 in the TNC

To detect whether there was a change in total glutamate concentration in CM group and sham group, the concentration of glutamate in the TNC was measured by HPLC. As shown in Table 1, the glutamate concentration in the CM group was significantly higher than that in the sham group. Then, q-PCR and Western blot were used to analyze the expression of EAAT2, and the results showed that the expression levels of EAAT2 in the CM group were decreased compared to that in the sham group (Fig. 4a, b, c). In addition, the double immunofluorescence staining revealed that EAAT2 was mainly expressed on astrocytes (Fig. 4d).

EAAT2 expression enhancers attenuated inflammatory soup-induced hyperalgesia and expression of CGRP in the TNC

EAAT2 is responsible for almost 90% of glutamate uptake. Two different EAAT2 expression enhancers (Cef, LDN-212320) were given to explore the effect of upregulating EAAT2 expression on cutaneous hyperalgesia and CGRP expression induced by repeated dura inflammatory soup stimulations. As shown in Fig. 5, the mechanical thresholds of periorbital and hind paw and the thermal thresholds of hind paw were significantly lower in the CM and CM+DMSO groups than those in the sham group. Intracerebroventricular injection of Cef (50 μg) did not change the pain thresholds or the expression of CGRP in the CM group. However, high doses of Cef (200 μg) greatly improved the mechanical and thermal pain thresholds and decreased the expression of CGRP in the CM group. Compared with Cef, LDN-212320 at doses of 5 μg and 20 μg were both capable of upregulating EAAT2 expression, elevating the pain thresholds in the CM group and restoring CGRP to a normal expression levels. Since 5 μg of LDN-212320 achieved the same effect as 200 μg of Cef and had a significant protective effect on allodynia, LDN-212320 (5 μg)

was chosen for subsequent experiments (Fig. 5).

LDN-212320 attenuated the expression of CGRP and SP in the TNC of CM rats

CGRP and SP, synthesized and released by primary afferent neurons, are key neuropeptide substances in the trigeminovascular system (TGVS). Persistent peripheral noxious stimulation increases the release of CGRP and SP, enhances the transmission of nociceptive signals and induces hyperalgesia (Tajti *et al.* 2015; Iyengar *et al.* 2017). To investigate whether upregulation of EAAT2 expression could attenuate the transmission of nociceptive signals, expression of CGRP and SP in the TNC was examined. The Western blots showed that the expression of CGRP in the CM and CM+DMSO groups was significantly higher than that in the sham group. Administration of LDN-212320 highly attenuated the increase in CGRP induced by inflammatory soup infusions (Fig. 6a, b). Then, the immunoreactivity of CGRP and SP in the TNC were evaluated by immunofluorescence staining (Fig. 6c). The fluorescence intensity of CGRP and SP in the CM group was higher than that in sham group, and treatment with LDN-212320 weakened the increase in CGRP and SP immunoreactivity (Fig. 6d, e).

Repeated dural stimulations activated astrocytes in the TNC

To investigate whether changes in astrocyte response are involved in the pathogenesis of CM, a semi-quantitative immunofluorescence analysis of GFAP (a specific marker for astrocytes) was performed in the TNC (Fig. 7). In the analysis areas, the ratio of GFAP-positive cells to the total cells in the CM and CM+DMSO groups was significantly increased compared with the sham group. Interestingly, administration of LDN-212320 inhibited the proliferation of astrocytes in the TNC of CM rats (Fig. 7e). In terms of morphology, astrocytes in the CM and CM+DMSO groups seemed to be hypertrophic compared with the sham group (Fig. 7a'-d').

EAAT2 expression enhancer LDN-212320 decreased the glutamate concentration and the expression of phosphorylated NR2B at tyrosines 1472 and 1474 in the TNC

The increased glutamate concentration could lead to overactivation of NMDA receptors, and phosphorylation of NMDA receptors is a key factor in stimulating and maintaining central sensitization. To investigate whether upregulation of EAAT2 expression could attenuate excessive activation of glutamate receptors by reducing the accumulation of glutamate in the TNC, the glutamate concentration and tyrosine phosphorylation of NR2B (pNR2B-Y1472 and pNR2B-Y1474) in CM rats were measured after administration of LDN-212320. Treatment with

LDN-212320 decreased the glutamate concentration and the expression of pNR2B-Y1472 and pNR2B-Y1474 in CM rats, and no significant difference was found in tNR2B expression among the groups (Table 1, Fig. 8).

Upregulation of EAAT2 expression reduced synaptic plasticity in CM rats

Our previous study found that phosphorylation of NR2B participated in the pathogenesis of CM by regulating synaptic plasticity (Wang *et al.* 2018). In addition, since our study revealed that upregulation of EAAT2 inhibited the phosphorylation expression of NR2B, to further explore whether EAAT2 regulated synaptic plasticity in CM rats, we examined the expression of synaptic-associated proteins Syp, Syt-1 and PSD95 in the TNC. Postsynaptic density (PSD) is a special structure located in the central nervous system's postsynaptic membrane and is the key material of postsynaptic signal transduction and integration (Ehrlich *et al.* 2007). Syp is a synaptic vesicle protein closely related to the function and structure of synapses and is widely used as a marker of synaptic activity(Valtorta *et al.* 2004). Syt-1 presents on the vesicle membranes of nerves and endocrine cells and is considered to be the major Ca^{2+} receptor in the process of cell secretion and is a marker of synaptic transmission (Poskanzer *et al.* 2003). Western blot analysis revealed that the expression of Syp, Syt-1 and PSD95 in the CM and CM+DMSO groups was significantly increased compared with the sham group, and administration of LDN-212320 reduced their expression. In addition, no difference was found in the expression of Syp, Syt-1 and PSD95 between the sham group and the sham+LDN-212320 group, indicating that LDN-212320 itself did not affect the synaptic plasticity (Fig. 9).

The expression of EAAT2 regulated the ultrastructure of synapses observed by transmission electron microscopy

The changes in the synaptic ultrastructure of the TNC neurons in each group were observed under TEM (Fig. 10). In the sham group and the sham+LDN-212320 group, the synaptic cleft was clearly visible, and the presynaptic membrane was clear and uniform with a complete outline. Numerous synaptic vesicles were observed in the anterior membrane region, and abundant PSD was detected in the posterior membrane. On the other hand, the synaptic space in the CM and CM+DMSO groups were widened and blurred. The thickness of postsynaptic densities, the curvature of the synaptic interface and the length of active regions were increased as well. Administration of LDN-212320 restored the indicators of morphological changes to the synapse (Table 2).

The regulation of EAAT2 expression on the number of dendritic spines in neurons observed by Golgi-Cox

staining

The dendritic spines of the pyramidal neurons in the TNC region were quantified using Golgi-Cox staining (Fig. 11). Data analysis showed that increased dendritic spine densities were observed in the CM and CM+DMSO groups compared with the sham group and sham+LDN-212320 group, and there was no statistical difference between sham group and sham+LDN-212320 group. Injection of LDN-212320 reduced the density of dendritic spines, indicating an increase in synaptic transmission efficiency in CM rats that was closely related to EAAT2 expression.

Upregulation of EAAT2 expression attenuated central sensitization in CM rats

To investigate whether EAAT2 is involved in the CM central sensitization process, the expression of proteins associated with central sensitization were examined. Activation of c-Fos and phosphorylation of CREB have been used as reliable markers of neuronal activation and central sensitization (Harris 1998; Liang *et al.* 2016; Anderson & Seybold 2000). Our results revealed that the expression levels of c-Fos and phosphorylated CREB (pCREB-S133, pCREB-S129) in the CM and CM+DMSO groups were significantly higher than those in the sham group. Treatment with LDN-212320 reduced the expression of c-Fos and phosphorylated CREB, demonstrating that upregulation of EAAT2 expression attenuated central sensitization in CM rats. And there was no difference in the expression of central sensitization-related proteins (c-Fos and phosphorylated CREB) between the sham group and the sham+LDN-212320 group, indicating that LDN-212320 itself had no effect on neuronal excitability (Fig. 12).

Discussion

In the present study, EAAT2 expression levels were decreased in the a rat model of CM. The novel compound LDN-212320 could restore the protein expression of EAAT2 through translation activation, and upregulation of the EAAT2 attenuated allodynia and alleviated central sensitization by regulating synaptic plasticity in CM rats. A neuroprotective effect was obtained by the treatment with LDN-212320, indicating that the recovery of EAAT2 expression may be a new strategy for the treatment of CM, and LDN-212320 could be a potential therapeutic drug.

Animal model of CM

Migraine is known to be more prevalent in women and abundant evidence showed the role of estrogen in migraine pathogenesis (Chai *et al.* 2014; Allais *et al.* 2018). Since the estrogen levels of male animals are more stable than that

of female animals, in order to exclude the influence of estrogen levels fluctuation, the male rats were chosen in our study.

A seven-day repeated dural inflammatory soup infusions were conducted to build a CM animal model in our study. As a recognized and reliable animal model of CM, persistent peripheral nociceptive stimulations can activate the trigeminal neurovascular system and lead to hyperalgesia or allodynia, imitating the common symptoms of CM patients(Melo-Carrillo & Lopez-Avila 2013). After the repeated inflammatory soup infusions, rats in the CM group exhibited reduced mechanical pain thresholds and thermal pain thresholds, which remained decreased in the next three days after the last inflammatory soup infusion. CGRP is a pain signal neuropeptide of the trigeminal nervous system that can be used as a biological indicator for diagnosing CM(Ramon *et al.* 2017; Cernuda-Morollon *et al.* 2013). The protein expression levels of CGRP in CM rats were significantly elevated compared with rats in the sham group. Both results of behavioral and biomarker indicated that a pain model associated with CM was successfully built after continuous inflammatory soup stimulations.

CM and EAAT2

Glutamate has long been considered to be involved in the pathogenesis of CM. Considering its excitatory effects on nociceptive neurons along the trigeminovascular pathway, the role of glutamate as a pivotal neurotransmitter in the procession of migraine-related central sensitization cannot be ignored (Hoffmann & Charles 2018).

Low concentrations of glutamate in the synaptic cleft ensures normal transmission of incoming signals. A large amount of pre-clinical and clinical evidence indicated that CM patients have increased glutamate levels in peripheral blood (Ferrari *et al.* 2009), saliva (Nam *et al.* 2018; Rajda *et al.* 1999), cerebrospinal fluid (Vieira *et al.* 2007), and the occipital cortex (Zielman *et al.* 2017) during headache and interictal periods. In our study, HPLC was used to detect the glutamate concentration in the TNC, which was significantly higher in the CM group than in the sham group, indicating that abnormal glutamate concentration was involved in the pathogenesis of CM.

EAAT2 plays a critical role in the clearance of extracellular glutamate and precisely regulated the glutamate concentration in the synaptic cleft (Takahashi *et al.* 2015a). The excitotoxicity of glutamate caused by EAAT2 dysfunction has been involved in a variety of neurodegenerative diseases, such as stroke, amyotrophic lateral sclerosis (ALS), Alzheimer's disease and epilepsy, among others (Takahashi *et al.* 2015a). Similarly, in our study of CM rats,

EAAT2 mRNA and protein expression were significantly downregulated. Although EAAT2 is of paramount importance in regulating the excitotoxicity of neurological diseases, the practical drugs that can be used in clinical treatment are limited.

Cef is an FDA-approved beta-lactam antibiotic that increases EAAT2 expression through transcriptional activation mechanism. In an animal model of ALS, Cef had neuroprotective effects in vitro and in vivo by increasing the expression of EAAT2. However, a large clinical trial was conducted to test the efficacy of ceftriaxone in ALS patients, but was stopped because it did not meet the predetermined therapeutic criteria (Fontana 2015). This disappointing result led us to consider whether Cef could effectively increase the expression of EAAT2 's functional membrane protein. Since elevation of the overall expression levels of EAAT2 usually does not match the corresponding increase in EAAT2-mediated glutamate uptake activity, an increase in EAAT2 expression on the plasma membrane of astrocytes is critical for glutamate uptake (Foran *et al.* 2014).

Recently, Kong and colleagues described a novel compound, LDN-212320, which effectively increases the expression of EAAT2 in plasma membrane by enhancing the translation mechanism (Kong *et al.* 2014). In primary neuron-astrocyte co-cultures, LDN-212320 protected neurons from glutamate-induced excitotoxicity by enhancing glutamate uptake. In addition, treatment with LDN-212320 provided protective effects in a variety of animal models. For example, in an animal model of ALS, LDN-212320 delayed the decline of motor function and prolonged survival of ALS mice (Takahashi *et al.* 2015b). In epilepsy animal model, LDN-212320 reduced the mortality, neuronal death and spontaneous recurrent seizures (Kong *et al.* 2014). Also, LDN-212320 significantly attenuated nociceptive behavior in mice of formalin-induced pain (Alotaibi & Rahman 2019).

In our study, effects of both EAAT2 expression enhancers (Cef and LDN-212320) were explored in our animal model of CM. And it was found that LDN-212320 had better efficiency in upregulating EAAT2 protein expression and relieving allodynia in CM rats (5 μg of LDN-212320 achieved the same effect of 200 μg Cef). As the increased EAAT2 through LDN-212320 is mainly expressed in plasma membrane, the total protein expression of EAAT2 was detected in our experiment.

In our experiment, intraventricular injection of LDN-212320 reduced the glutamate concentration in the TNC of CM rats, and significantly decreased the expression of CGRP, reducing the transmission of nociceptive signals and alleviated the mechanical and thermal allodynia in CM rats. LDN-212320 showed a good ability in upregulating the

EAAT2 expression and the drug itself did not affect neuronal excitability. Compared with Cef, LDN-212320 has the advantages of non-toxicity, small molecular weight and better drug efficiency. These results opened the possibility that LDN-212320 is a therapeutic option for CM. However, the mechanism LDN-212320 upregulates EAAT2 expression is unclear. The study by (Kong *et al.* 2014) has found that treatment with LDN-212320 led the activation of PKC, which subsequently stimulated YB-1 (a nucleic acid‐binding protein that is important for translational regulation), and resulting in enhanced EAAT2 translation. Future study should focus on the molecular mechanism of EAAT2 translation activated by LDN-212320 and more behavioral tests (such as freezing behavior, exploration behavior, resting behavior) need to be carried out.

CM and central sensitization

Phosphorylation of NMDA receptors is the key molecular mechanism underlying the central sensitization, overactivated NMDA receptors would lead to an increase in the efficiency of glutamatergic neurotransmission, and the enhancement of neuronal synaptic plasticity is the basis for the initiation and maintenance of pain (Ji *et al.* 2003; Liu & Salter 2010). NR2B is the most important and broadly studied tyrosine phosphorylation protein of the NMDA receptors, in our previous study, inhibition of phosphorylated NR2B attenuated the central sensitization in CM rats by modulating synaptic plasticity (Wang *et al.* 2018). In our experiment, it was found that the restoration of EAAT2 protein expression inhibited the phosphorylation of NR2B. To explore whether upregulation of EAAT2 regulates synaptic plasticity by inhibiting phosphorylation of NR2B, silver staining and electron microscopy were used to observe structural changes in the synapse, and synapse-related proteins were analyzed by Western blot. The results from synaptic structure and synaptic-associated protein analyses showed that the synaptic plasticity of neurons in CM rats was significantly enhanced, while upregulation of EAAT2 expression restored neuronal synaptic plasticity to normal levels.

To further evaluate whether EAAT2 regulated the central sensitization process in CM rats, the expression levels of phosphorylated CREB and c-Fos were measured. CREB is involved in the sensitization of nociceptive cells and plays a role through phosphorylation (Anderson & Seybold 2000; Ma & Quirion 2001). Phosphorylated CREB leads to the activation of c-Fos, which has been widely used as a marker of neuronal activation in the nociceptive pathway (Mitsikostas *et al.* 2011; Harris 1998). In our experiment, treatment with LDN-212320 reduced the protein expression

of pCREB and c-Fos in CM rats, indicating that the upregulation of EAAT2 alleviated the hyperexcitability of neurons and ameliorated the central sensitization in CM rats

CM and astrocytes

Our understanding of pathological pain led us to focus on the neuronal mechanism. Considering neuronal activity alone cannot fully elucidate the production and maintenance of chronic neuropathic pain. Activation of glial cells and interactions with neurons are emerging as a potential mechanism (Loggia *et al.* 2015). Astrocytes are the most abundant glial cells in the CNS. Close contact with neurons and synapses enables astrocytes not only to support and nourish neurons but also to regulate the external chemicals environment during synaptic transmission (Singh & Abraham 2017). It is well-known that EAAT2 expressed on astrocytes can modulate synaptic plasticity of neurons by regulating glutamate concentration in the synaptic cleft through the glutamate-glutamine cycle. When the CNS is damaged, astrocytes can be activated, which is manifested by proliferation, hypertrophy, release of glial medium, and downregulation of glutamate transporters. Proliferation of spinal astrocytes has been demonstrated in neuropathic pain models, and injection of astrocyte inhibitor inhibited the proliferation of astrocytes and reduced neuropathic pain (Ji *et al.* 2013). In our experiment, we also found that after stimulation by inflammatory soup, astrocytes in the TNC proliferated and were hypertrophic. Notably, LDN-212320 reduced the activation of astrocytes, which may be the result of EAAT2 upregulation but may also be a direct LDN-212320 effect. The activation status of astrocytes we observed in CM rats implicated that astrocytes may be involved in the pathogenesis of CM. Understanding the molecular mechanism of cross-talk between TNC neurons and astrocytes may contribute to a deep understanding of CM. Therefore, the duration of astrocytes' reactivity in CM rats and the studies on the molecular mechanisms in astrocytes needs to be carried out in the follow-up experiments.

Conclusion

Our study demonstrated downregulated expression of EAAT2 in a rat model of CM, and that recovery of EAAT2 expression can reduce the transmission of nociceptive signals and regulate synaptic plasticity to alleviate central sensitization. Therefore, regulation of EAAT2 may provide a new therapeutic strategy for CM treatment and LDN-212320 may be a potential therapeutic drug.

Limitations of this experiment

Although an increase of the total glutamate level was detected in migraine patients and in our experiment, the glutamate concentration in the synaptic cleft is sensitive to the excitability of the neurons and will be more objective and rigorous if measured by microdialysis. Regarding synaptic plasticity, due to the lack of electrophysiological studies, we only explored the effects of experimental results on structural plasticity. Further studies on electrophysiology are needed to examine the effects on functional plasticity.

--Human subjects --

Involves human subjects:

If yes: Informed consent & ethics approval achieved:

=> if yes, please ensure that the info "Informed consent was achieved for all subjects, and the experiments were approved by the local ethics committee." is included in the Methods.

ARRIVE guidelines have been followed:

Yes

=> if it is a Review or Editorial, skip complete sentence => if No, include a statement in the "Conflict of interest disclosure" section: "ARRIVE guidelines were not followed for the following reason:

"

(edit phrasing to form a complete sentence as necessary).

=> if Yes, insert in the "Conflict of interest disclosure" section:

"All experiments were conducted in compliance with the ARRIVE guidelines." unless it is a Review or Editorial

Conflicts of interest: none

=> if 'none', insert "The authors have no conflict of interest to declare."

=> otherwise insert info unless it is already included

Acknowledgments

This work was supported by the National Natural Science Foundation of China (No: 81671093) and the District Science and Technology Projects of Yuzhong Chongqing (No: 20160107). The authors state that there is no potential conflict of interest in the study, authorship, and/or publication of this article. Xue Zhou conceived of and designed the research, performed the experiments, analyzed the data and wrote the manuscript. Li-Xue Chen wrote the proposal, conceived of the study, supervised the experiment and critically revised the manuscript. Ji-Ying Zhou provided useful advices on the design of this study. Jie Liang, Jiang Wang and Zhao-Yang Fei helped in the experiment of building the animal model and the data collecting. Guang-Cheng Qin and Dun-Ke Zhang helped in the immunofluorescence, electron microscope and silver staining experiments. All the authors read and approved the final manuscript.

References

Allais, G., Chiarle, G., Sinigaglia, S., Airola, G., Schiapparelli, P. and Benedetto, C. (2018) Estrogen, migraine, and vascular risk. *Neurol Sci* **39,** 11-20.

Alotaibi, G. and Rahman, S. (2019) Effects of glial glutamate transporter activator in formalin-induced pain behaviour in mice. *Eur J Pain* **23,** 765-783.

Anderson, L. E. and Seybold, V. S. (2000) Phosphorylated cAMP response element binding protein increases in neurokinin-1 receptor-immunoreactive neurons in rat spinal cord in response to formalin-induced nociception. *Neurosci Lett* **283,** 29-32.

Bernstein, C. and Burstein, R. (2012) Sensitization of the trigeminovascular pathway: perspective and implications to migraine pathophysiology. *J Clin Neurol* **8,** 89-99.

Boyko, M., Gruenbaum, S. E., Gruenbaum, B. F., Shapira, Y. and Zlotnik, A. (2014) Brain to blood glutamate scavenging as a novel therapeutic modality: a review. *J Neural Transm (Vienna)* **121,** 971-979.

Cernuda-Morollon, E., Larrosa, D., Ramon, C., Vega, J., Martinez-Camblor, P. and Pascual, J. (2013) Interictal increase of CGRP levels in peripheral blood as a biomarker for chronic migraine. *Neurology* **81,** 1191-1196.

Chai, N. C., Peterlin, B. L. and Calhoun, A. H. (2014) Migraine and estrogen. *Curr Opin Neurol* **27,** 315-324.

Chen, Y. L., Li, D., Wang, Z. Z., Xu, W. G., Li, R. P. and Zhang, J. D. (2016) Glutamate metabolism of astrocytes during hyperbaric oxygen exposure and its effects on central nervous system oxygen toxicity. *Neuroreport* **27,** 73-79.

Danbolt, N. C. (2001) Glutamate uptake. *Prog Neurobiol* **65,** 1-105.

Edvinsson, L. (2017) The Trigeminovascular Pathway: Role of CGRP and CGRP Receptors in Migraine. *Headache* **57 Suppl 2,** 47-55.

Ehrlich, I., Klein, M., Rumpel, S. and Malinow, R. (2007) PSD-95 is required for activity-driven synapse stabilization. *Proc Natl Acad Sci U S A* **104,** 4176-4181.

Ferrari, A., Spaccapelo, L., Pinetti, D., Tacchi, R. and Bertolini, A. (2009) Effective prophylactic treatments of migraine lower plasma glutamate levels. *Cephalalgia* **29,** 423-429.

Fontana, A. C. (2015) Current approaches to enhance glutamate transporter function and expression. *J Neurochem* **134,** 982-1007.

Foran, E., Rosenblum, L., Bogush, A., Pasinelli, P. and Trotti, D. (2014) Sumoylation of the astroglial glutamate transporter EAAT2 governs its intracellular compartmentalization. *Glia* **62,** 1241-1253.

Gegelashvili, G. and Bjerrum, O. J. (2014) High-affinity glutamate transporters in chronic pain: an emerging therapeutic target. *J Neurochem* **131,** 712-730.

Gegelashvili, G. and Bjerrum, O. J. (2019) Glutamate transport system as a key constituent of glutamosome: Molecular pathology and pharmacological modulation in chronic pain. *Neuropharmacology*.

Guldner, F. H. and Ingham, C. A. (1980) Increase in postsynaptic density material in optic target neurons of the rat suprachiasmatic nucleus after bilateral enucleation. *Neurosci Lett* **17,** 27-31.

Hargreaves, K., Dubner, R., Brown, F., Flores, C. and Joris, J. (1988) A new and sensitive method for measuring thermal nociception in cutaneous hyperalgesia. *Pain* **32,** 77-88.

Harris, J. A. (1998) Using c-fos as a neural marker of pain. *Brain Res Bull* **45,** 1-8.

He, W., Long, T., Pan, Q., Zhang, S., Zhang, Y., Zhang, D., Qin, G., Chen, L. and Zhou, J. (2019) Microglial NLRP3

inflammasome activation mediates IL-1beta release and contributes to central sensitization in a recurrent nitroglycerin-induced migraine model. *J Neuroinflammation* **16,** 78.

Hoffmann, J. and Charles, A. (2018) Glutamate and Its Receptors as Therapeutic Targets for Migraine. *Neurotherapeutics* **15,** 361-370.

Iyengar, S., Ossipov, M. H. and Johnson, K. W. (2017) The role of calcitonin gene-related peptide in peripheral and central pain mechanisms including migraine. *Pain* **158,** 543-559.

Izzo, P. N. and Bolam, J. P. (1988) Cholinergic synaptic input to different parts of spiny striatonigral neurons in the rat. *J Comp Neurol* **269,** 219-234.

Ji, R. R., Berta, T. and Nedergaard, M. (2013) Glia and pain: is chronic pain a gliopathy? *Pain* **154 Suppl 1,** S10-28.

Ji, R. R., Kohno, T., Moore, K. A. and Woolf, C. J. (2003) Central sensitization and LTP: do pain and memory share similar mechanisms? *Trends Neurosci* **26,** 696-705.

Jones, D. G. and Devon, R. M. (1978) An ultrastructural study into the effects of pentobarbitone on synaptic organization. *Brain Res* **147,** 47-63.

Kobayashi, A., Parker, R. L., Wright, A. P., Brahem, H., Ku, P., Oliver, K. M., Walz, A., Lester, H. A. and Miwa, J. M. (2014) Lynx1 supports neuronal health in the mouse dorsal striatum during aging: an ultrastructural investigation. *J Mol Neurosci* **53,** 525-536.

Kong, Q., Chang, L. C., Takahashi, K. et al. (2014) Small-molecule activator of glutamate transporter EAAT2 translation provides neuroprotection. *J Clin Invest* **124,** 1255-1267.

Latremoliere, A. and Woolf, C. J. (2009) Central sensitization: a generator of pain hypersensitivity by central neural plasticity. *J Pain* **10,** 895-926.

Li, Q., Clark, S., Lewis, D. V. and Wilson, W. A. (2002) NMDA receptor antagonists disinhibit rat posterior cingulate and retrosplenial cortices: a potential mechanism of neurotoxicity. *J Neurosci* **22,** 3070-3080.

Liang, Y., Liu, Y., Hou, B., Zhang, W., Liu, M., Sun, Y. E., Ma, Z. and Gu, X. (2016) CREB-regulated transcription coactivator 1 enhances CREB-dependent gene expression in spinal cord to maintain the bone cancer pain in

mice. *Mol Pain* **12**.

Lipton, R. B., Bigal, M. E., Diamond, M., Freitag, F., Reed, M. L., Stewart, W. F. and Group, A. A. (2007) Migraine prevalence, disease burden, and the need for preventive therapy. *Neurology* **68,** 343-349.

Liu, C., Zhang, Y., Liu, Q. et al. (2018) P2X4-receptor participates in EAAT3 regulation via BDNF-TrkB signaling in a model of trigeminal allodynia. *Mol Pain* **14,** 1744806918795930.

Liu, X. J. and Salter, M. W. (2010) Glutamate receptor phosphorylation and trafficking in pain plasticity in spinal cord dorsal horn. *Eur J Neurosci* **32,** 278-289.

Loggia, M. L., Chonde, D. B., Akeju, O. et al. (2015) Evidence for brain glial activation in chronic pain patients. *Brain* **138,** 604-615.

Ma, W. and Quirion, R. (2001) Increased phosphorylation of cyclic AMP response element-binding protein (CREB) in the superficial dorsal horn neurons following partial sciatic nerve ligation. *Pain* **93,** 295-301.

Mathew, N. T. (2011) Pathophysiology of chronic migraine and mode of action of preventive medications. *Headache* **51 Suppl 2,** 84-92.

Melo-Carrillo, A. and Lopez-Avila, A. (2013) A chronic animal model of migraine, induced by repeated meningeal nociception, characterized by a behavioral and pharmacological approach. *Cephalalgia* **33,** 1096-1105.

Mitsikostas, D. D., Knight, Y. E., Lasalandra, M., Kavantzas, N. and Goadsby, P. J. (2011) Triptans attenuate capsaicin-induced CREB phosphorylation within the trigeminal nucleus caudalis: a mechanism to prevent central sensitization? *J Headache Pain* **12,** 411-417.

Nam, J. H., Lee, H. S., Kim, J., Kim, J. and Chu, M. K. (2018) Salivary glutamate is elevated in individuals with chronic migraine. *Cephalalgia* **38,** 1485-1492.

Perez-Cruz, C., Simon, M., Flugge, G., Fuchs, E. and Czeh, B. (2009) Diurnal rhythm and stress regulate dendritic architecture and spine density of pyramidal neurons in the rat infralimbic cortex. *Behav Brain Res* **205,** 406-413.

Poskanzer, K. E., Marek, K. W., Sweeney, S. T. and Davis, G. W. (2003) Synaptotagmin I is necessary for compensatory

synaptic vesicle endocytosis in vivo. *Nature* **426,** 559-563.

Rajda, C., Tajti, J., Komoroczy, R., Seres, E., Klivenyi, P. and Vecsei, L. (1999) Amino acids in the saliva of patients with migraine. *Headache* **39,** 644-649.

Ramon, C., Cernuda-Morollon, E. and Pascual, J. (2017) Calcitonin gene-related peptide in peripheral blood as a biomarker for migraine. *Curr Opin Neurol* **30,** 281-286.

Rao, P., Yallapu, M. M., Sari, Y., Fisher, P. B. and Kumar, S. (2015) Designing Novel Nanoformulations Targeting Glutamate Transporter Excitatory Amino Acid Transporter 2: Implications in Treating Drug Addiction. *J Pers Nanomed* **1,** 3-9.

Singh, A. and Abraham, W. C. (2017) Astrocytes and synaptic plasticity in health and disease. *Exp Brain Res* **235,** 1645-1655.

Tajti, J., Szok, D., Majlath, Z., Tuka, B., Csati, A. and Vecsei, L. (2015) Migraine and neuropeptides. *Neuropeptides* **52,** 19-30.

Takahashi, K., Foster, J. B. and Lin, C. L. (2015a) Glutamate transporter EAAT2: regulation, function, and potential as a therapeutic target for neurological and psychiatric disease. *Cell Mol Life Sci* **72,** 3489-3506.

Takahashi, K., Kong, Q., Lin, Y. et al. (2015b) Restored glial glutamate transporter EAAT2 function as a potential therapeutic approach for Alzheimer's disease. *J Exp Med* **212,** 319-332.

Tfelt-Hansen, P. and Olesen, J. (2012) Taking the negative view of current migraine treatments: the unmet needs. *CNS Drugs* **26,** 375-382.

Valtorta, F., Pennuto, M., Bonanomi, D. and Benfenati, F. (2004) Synaptophysin: leading actor or walk-on role in synaptic vesicle exocytosis? *Bioessays* **26,** 445-453.

Vieira, D. S., Naffah-Mazzacoratti Mda, G., Zukerman, E., Senne Soares, C. A., Cavalheiro, E. A. and Peres, M. F. (2007) Glutamate levels in cerebrospinal fluid and triptans overuse in chronic migraine. *Headache* **47,** 842-847.

Wang, X. Y., Zhou, H. R., Wang, S., Liu, C. Y., Qin, G. C., Fu, Q. Q., Zhou, J. Y. and Chen, L. X. (2018) NR2B-Tyr

phosphorylation regulates synaptic plasticity in central sensitization in a chronic migraine rat model. *J Headache Pain* **19,** 102.

Weissgerber, T. L., Milic, N. M., Winham, S. J. and Garovic, V. D. (2015) Beyond bar and line graphs: time for a new data presentation paradigm. *Plos Biol* **13,** e1002128.

Willard, S. S. and Koochekpour, S. (2013) Glutamate, glutamate receptors, and downstream signaling pathways. *Int J Biol Sci* **9,** 948-959.

Woolf, C. J. and Thompson, S. W. (1991) The induction and maintenance of central sensitization is dependent on N-methyl-D-aspartic acid receptor activation; implications for the treatment of post-injury pain hypersensitivity states. *Pain* **44,** 293-299.

Zhou, H., Wang, X., Wang, S., Liu, C., Fu, Q., Qin, G., Zhou, J. and Chen, L. (2019) Inhibition of Nerve Growth Factor Signaling Alleviates Repeated Dural Stimulation-induced Hyperalgesia in Rats. *Neuroscience* **398,** 252-262.

Zielman, R., Wijnen, J. P., Webb, A., Onderwater, G. L. J., Ronen, I., Ferrari, M. D., Kan, H. E., Terwindt, G. M. and Kruit, M. C. (2017) Cortical glutamate in migraine. *Brain* **140,** 1859-1871.

Picture annotation:

Fig. 1

The time-line and experimental procedures of this study. Rats were acclimatized for one week and assigned to each experimental group after a simple randomization (6~10 rats per group). At day 8, a total of 205 rats underwent surgery and 9 rats were excluded due to dural damage during the surgery. Then, rats were recovered for one week to the pre-operative levels (4 rats were excluded due to the infection and 2 rats were excluded due to the pain thresholds didn't return to the pre-operative levels). Rats that recovered to the pre-operative levels received a 7-day dura infusions and behavioral tests (n = 10 rats per group). Next, rats were administrated with drugs and the behaviors were tested (n = 10 rats per group). Last step, 24 hours after the administrations, rats were sacrificed for the following HPLC, q-RCR, Western blot, IF, TEM, Golgi-cox experimental studies (n = 6 rats per group).

Fig.2

Schematic representation of the brain region for TNC.

The white dotted frame represents the TNC regions (Liu *et al.* 2018) and the white solid line rectangular box in the TNC areas were selected for the analysis of astrocytes. Nuclei were labeled with DAPI (blue), and astrocytes were labeled with GFAP (red).

Fig. 3

Pain thresholds and expression of CGRP in TNC after repeated IS or PBS infusions. a. Schematic diagram of infusion time. b-c. Repeated dural inflammatory soup infusions reduced the mechanical pain threshold of hind paw and periorbital area of rats, and induced hyperalgesia in rats of the CM group. d. The thermal pain threshold of the hind paw in the inflammatory soup group was similar to the mechanical pain threshold and was much lower than that of the PBS group on the third day. e. After 7 days of continuous infusions, the inflammatory soup group showed increased expression of CGRP in the TNC. f. The statistical analysis result was presented in box-plots, the box dimension shows the median and interquartile range, the center line show the median and the box limits indicate the 25th and 75th percentiles and the whiskers shows the remaining 50% of the data range ($n = 10$ rats per group, $^*P < 0.05$ compared with the sham group). Protein expression in the bar graphs is shown relative to the intensity beta-actin/GAPDH.

Fig. 4

The localization of EAAT2 and the expression levels in the TNC. a-b. EAAT2 protein expression in the TNC of the CM group was remarkably decreased compared to that in the sham group. Protein expression in the bar graphs is shown relative to the intensity beta-actin/GAPDH. c. EAAT2 mRNA expression in the TNC of the CM group was consistent with EAAT2 protein expression and was also significantly decreased ($n = 6$ rats per group, $^*P < 0.05$ compared with the sham group). d. Double immunofluorescence staining of GFAP (green) with EAAT2 (red) in the TNC. EAAT2 was mainly expressed on astrocytes (shown by arrows) ($n = 3$ rats, 5 pictures per rats, scale bar = 20 μm). The statistical analysis results were presented in box-plots, the box dimension shows the median and

interquartile range, the center line show the median and the box limits indicate the 25th and 75th percentiles and the whiskers shows the remaining 50% of the data range.

Fig. 5

Effects of two EAAT2 expression enhancers on pain thresholds and protein expression of EAAT2 and CGRP in CM rats. a-c. The mechanical and thermal pain thresholds of the periorbital and hindpaw in each experimental group. Rats in CM+Cef (200 μg), CM+LDN-212320 (5 μg) and CM+LDN-212320 (20 μg) groups had higher pain thresholds of the periorbital and hindpaw compared with those in CM, CM+DMSO and CM+Cef (50 μg) groups (n = 10 rats per group, $P < 0.05$, *P vs sham group; #P vs CM+DMSO group). d-f. The protein expression of EAAT2 and CGRP in each experimental group. Treatment with Cef (200 μg), LDN-212320 (5 μg) and LDN-212320 (20 μg) restored EAAT2 to normal expression levels and downregulated CGRP expression, and there was no statistical difference of EAAT2 and CGRP protein expression in CM, CM + DMSO and CM+Cef (50 μg) groups (n = 6 rats per group, $P < 0.05$, *P vs sham group; #P vs CM+DMSO group). The statistical analysis results were presented in box-plots, the box dimension shows the median and interquartile range, the center line show the median and the box limits indicate the 25th and 75th percentiles and the whiskers shows the remaining 50% of the data range. Protein expression in the bar graphs is shown relative to the intensity beta-actin/GAPDH.

Fig. 6

The protein expression of CGRP and immunofluorescence staining of CGRP and SP in the TNC. a-b. Compared with the sham group, the protein expression of CGRP in the CM and CM+DMSO groups was highly increased, and administration of LDN-212320 recovered the expression of CGRP to normal expression levels (n = 6 rats per group, $P < 0.05$, *P vs Sham group; #P vs CM+DMSO group). Protein expression in the bar graphs is shown relative to the intensity beta-actin/GAPDH. c-e The immunofluorescence staining showed that the fluorescence intensity of CGRP and SP in the CM and CM+DMSO groups was significantly higher than that in sham group, and treatment with LDN-212320 alleviated the increase of CGRP and SP fluorescence intensity in CM rats (n = 6 rats per group, $P < 0.05$, *P vs Sham group; #P vs CM+DMSO group, scale bar = 200 μm). The statistical analysis results were presented in

box-plots, the box dimension shows the median and interquartile range, the center line show the median and the box limits indicate the 25th and 75th percentiles and the whiskers shows the remaining 50% of the data range.

Fig. 7

Effect of repeated dural inflammatory soup stimulations on the astrocyte response in the TNC. a, sham group; b, CM group; c, CM+DMSO group; d, CM+LDN-212320 group. a'-d'. Magnified images of a-d. a'-d'. Morphologically, astrocytes were observed under a 40× objective, the CM and CM+DMSO groups showed hypertrophy compared with the sham group, and administration of LDN-212320 restored the morphology of astrocytes to normal. e. The ratio of the number of astrocytes (labeled by GFAP) to the number of total cells (labeled by DAPI) was analyzed under a 20× objective. Compared with the sham group, inflammatory soup stimulations increased the percentage of astrocyte cells, and treatment with LDN-212320 alleviated the proliferation of astrocytes. ($n = 6$ rats per group, $P < 0.05$, *P vs sham group; #P vs CM+DMSO group, scale bars = 100 μm (a-d), scale bars = 20 μm (a'-d'). The statistical analysis result was presented in box-plots, the box dimension shows the median and interquartile range, the center line show the median and the box limits indicate the 25th and 75th percentiles and the whiskers shows the remaining 50% of the data range.

Fig. 8

Expression of phosphorylated NR2B (pNR2B-Y1472 and pNR2B-Y474) and tNR2B in each group. a-c. Immunoblotting bands of tNR2B, pNR2B-Y1472, pNR2B-Y1474 and β-actin. d. There was no significant difference in the expression of tNR2B in each group. e-f. Expression of pNR2B-Y1472 and pNR2B-Y1474 in the CM and CM+DMSO group was significantly higher than that in the sham group, and treatment with LDN-212320 decreased the expression of pNR2B-Y1472 and pNR2B-Y1474 in the TNC. ($n = 6$ rats per group, $P < 0.05$, *P vs sham group; #P vs CM+DMSO group). The statistical analysis results were presented in box-plots, the box dimension shows the median and interquartile range, the center line show the median and the box limits indicate the 25th and 75th percentiles and the whiskers shows the remaining 50% of the data range. Protein expression in the bar graphs is shown relative to the intensity beta-actin/GAPDH.

Fig. 9

Expression of the synaptic-associated proteins Syp, Syt-1 and PSD95 in the TNC. a-f. Protein expression of Syp, Syt-1 and PSD95 in the TNC was increased in the CM and CM+DMSO groups compared with that in the sham group, administration of LDN-212320 decreased the expression of Syp, Syt-1 and PSD95 in CM rats. e-l. There was no significant difference in the expression of Syp, Syt-1 and PSD95 bewteen the sham group and the sham+LDN-212320 group. (n = 6 rats per group, $P < 0.05$, *P vs sham group; #P vs CM+DMSO group). The statistical analysis results were presented in box-plots, the box dimension shows the median and interquartile range, the center line show the median and the box limits indicate the 25th and 75th percentiles and the whiskers shows the remaining 50% of the data range. Protein expression in the bar graphs is shown relative to the intensity beta-actin/GAPDH.

Fig. 10

The changes in the synaptic ultrastructure of the TNC neurons in each group were observed under TEM. a-e.Ultrastructure of synapses in each group (a, sham group; b, CM group; c, CM+DMSO group; d, CM+LDN-212320 group; e, sham+LDN-212320 group, scale bar =200 nm). a'-e'. Magnified images of a-e (a', sham group; b', CM group; c', CM+DMSO group; d', CM+LDN-212320 group; e, sham+LDN-212320 group, scale bar = 80 nm). PSD, postsynaptic density; SC, synaptic cleft; SV, synaptic vesicle (n = 6 rats per group, 10 images per rats were arbitrarily taken, $P < 0.05$, *P vs sham group; #P vs CM+DMSO group).

Fig.11

Density of dendritic spines in TNC neurons. a-e. Morphology of pyramidal neurons in each group (a, sham group; b, CM group; c, CM+DMSO group; d, CM+LDN-212320 group; e, sham+LDN-212320 group, scale bar = 20 μm). a'-e'. Magnified images of neurons to analyze the density of dendritic spines per 20 μm (a', sham group; b', CM group; c', CM+DMSO group; d', CM+LDN-212320 group; e', sham+LDN-212320 group, scale bar = 4 μm). f. Data analysis showed that increased dendritic spine densities were observed in CM and CM+ DMSO groups compared with sham

group, and there was no significant difference between CM and CM+DMSO groups. Administration of LDN-212320 reduced the density of dendritic spines, and no statistical difference was found between the sham group and the sham+LDN-212320 group (n = 6 rats per group, 5 images per rats were arbitrarily taken, $P < 0.05$, *P vs sham group; #P vs CM+DMSO group). The statistical analysis result was presented in box-plots, the box dimension shows the median and interquartile range, the center line show the median and the box limits indicate the 25th and 75th percentiles and the whiskers shows the remaining 50% of the data range. Protein expression in the bar graphs is shown relative to the intensity beta-actin/GAPDH.

Fig. 12

Expression of the central sensitization-associated proteins p-CREB-S129, t-CREB, p-CREB-S133, and c-Fos in the TNC. a-h. Expression of p-CREB-S129, p-CREB-S133, and c-Fos in the CM and CM+DMSO groups was significantly increased compared to the sham group, and treatment with LDN-212320 reduced the expression of these proteins. There was no difference in tCREB expression among groups. i-n. In addition, there was no statistical difference in the expression of p-CREB-S129, p-CREB-S133, and c-Fos in the sham and the sham+LDN-212320 groups (n = 6 rats per group, $P < 0.05$, *P vs sham group; #P vs CM+DMSO group). The statistical analysis results were presented in box-plots, the box dimension shows the median and interquartile range, the center line show the median and the box limits indicate the 25th and 75th percentiles and the whiskers shows the remaining 50% of the data range. Protein expression in the bar graphs is shown relative to the intensity beta-actin/GAPDH.

Fig.13

Schematic diagram of the astrocyte excitatory amino acid transporter 2 (EAAT2) participating in central sensitization process through modulating synaptic plasticity. Central sensitization is the potential pathogenesis of chronic migraine (CM) and is related to the persistent neuronal hyperexcitability. In our study, downregulated EAAT2 was found in CM rats, which may contribute to central sensitization by leading the accumulation of extracellular glutamate and enhancing the synaptic plasticity. The novel compound LDN-212320 greatly upregulated the protein expression of EAAT2, alleviated hyperalgesia, decreased the glutamate concentration and provided a neuroprotective effect in CM

rats, indicating that the recovery of EAAT2 expression may be a new strategy for the treatment of CM, and LDN-212320 could be a potential therapeutic drug.

Table 1

Glutamate concentration in the TNC of rats

Group(n=6 rats)	**Glutamate concentration (mg/g)**
sham	0.57±0.5909
CM	0.78±0.2999*
CM+DMSO	0.75±0.4628*
CM+LDN-212320	0.55±0.6757$^{\#}$

The glutamate concentration in the CM group and the CM+DMSO group was significantly increased compared with the sham group, and it was decreased after the treatment with LDN-212320. Data are presented as the mean ± SD. $P < 0.05$, *P vs sham group, $^{\#}$P vs CM+DMSO group, n = 6 rats per group.

Table 2

Synaptic morphological parameters in the TNC of rats

n=6 rats per group	**sham**	**CM**	**CM+DMSO**	**CM+LDN-212320**	**sham+LDN-212320**
Thickness of the PSD/nm	14.32±1.3206	45.50±4.9798*	46.77±4.4873*	20.21±1.4771$^{\#}$	16.27±3.4063$^{\#}$

Width of the synaptic cleft/nm	19.29±1.2399	30.07±3.532*	28.86±0.9860*	22.69±1.3576#	20.98±2.1810#
Synapticinterface curvature	1.08±0.0097	1.32±0.5317*	1.26±0.3396*	1.11±0.0399#	1.07±0.3257#
Active zones/nm	311±21.3528	512.60±48.1851*	498.02±49.4603*	329.20±41.4636#	320.23±32.0048#

The Thickness of the PSD, width of the synaptic cleft, synapticinterface curvature, and active zones in the CM group and the CM+DMSO group were significantly increased compared with the sham group, while treatment with LDN-212320 restored them to the normal expression levels. In addition, there was no statistical among the sham, CM+LDN-212320 and sham+LDN-212320 groups. Data are presented as the mean ± SD. $P < 0.05$, *P vs sham group; #P vs CM+DMSO group, n = 6 rats per group.

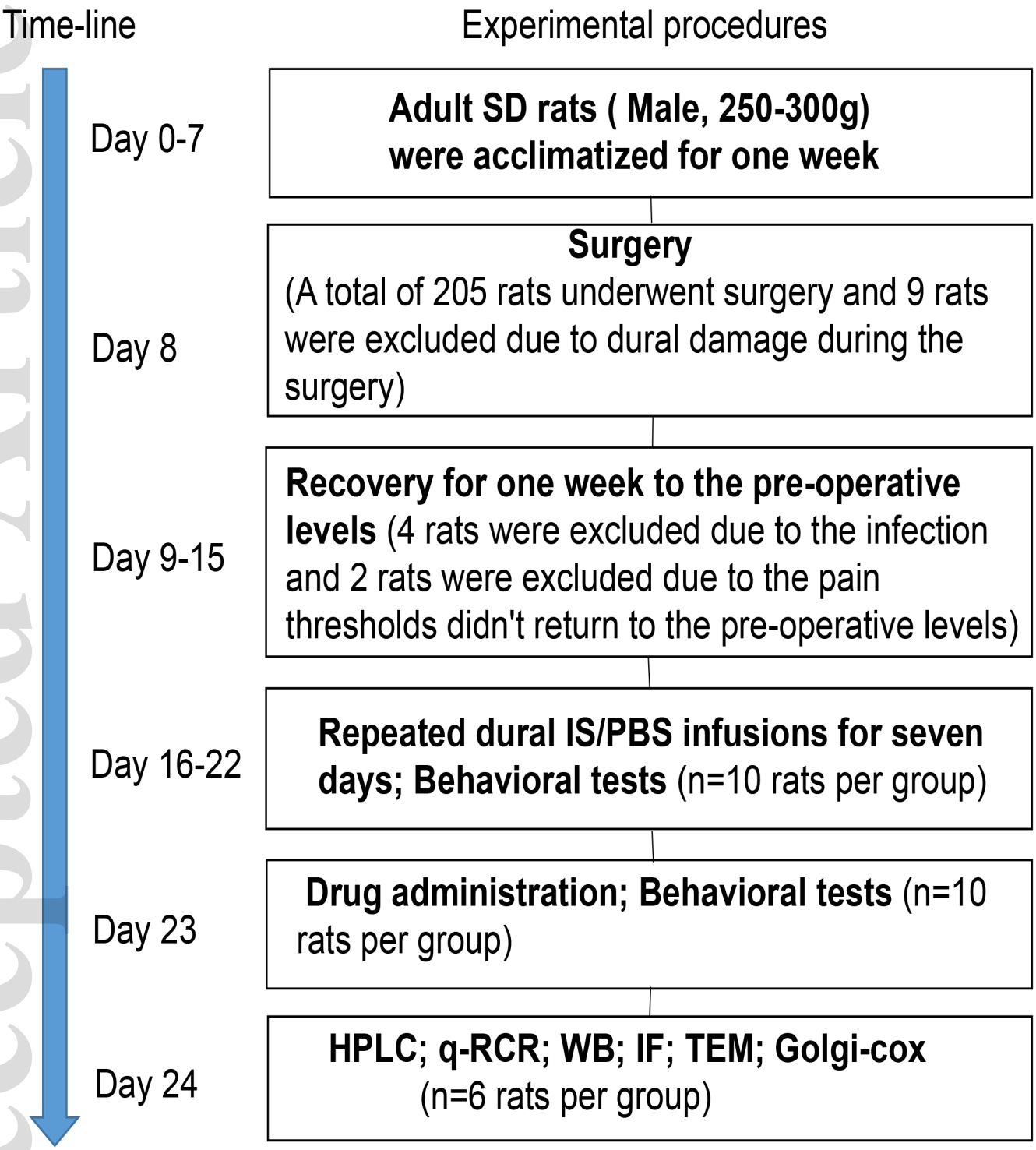

jnc_14944_f1.tif

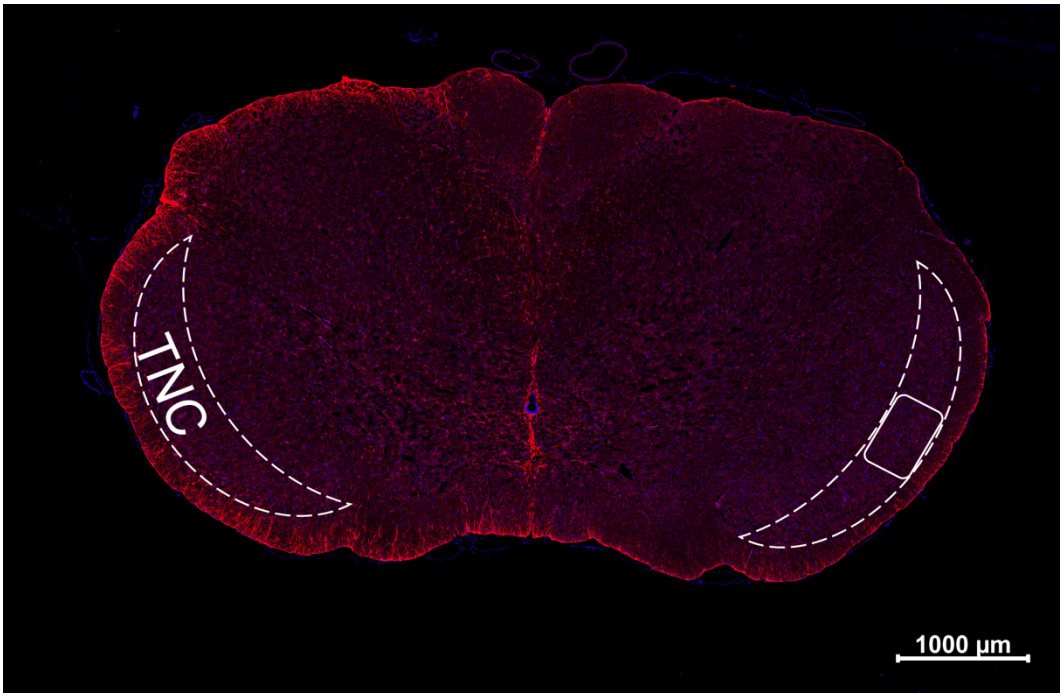

jnc_14944_f2.tif

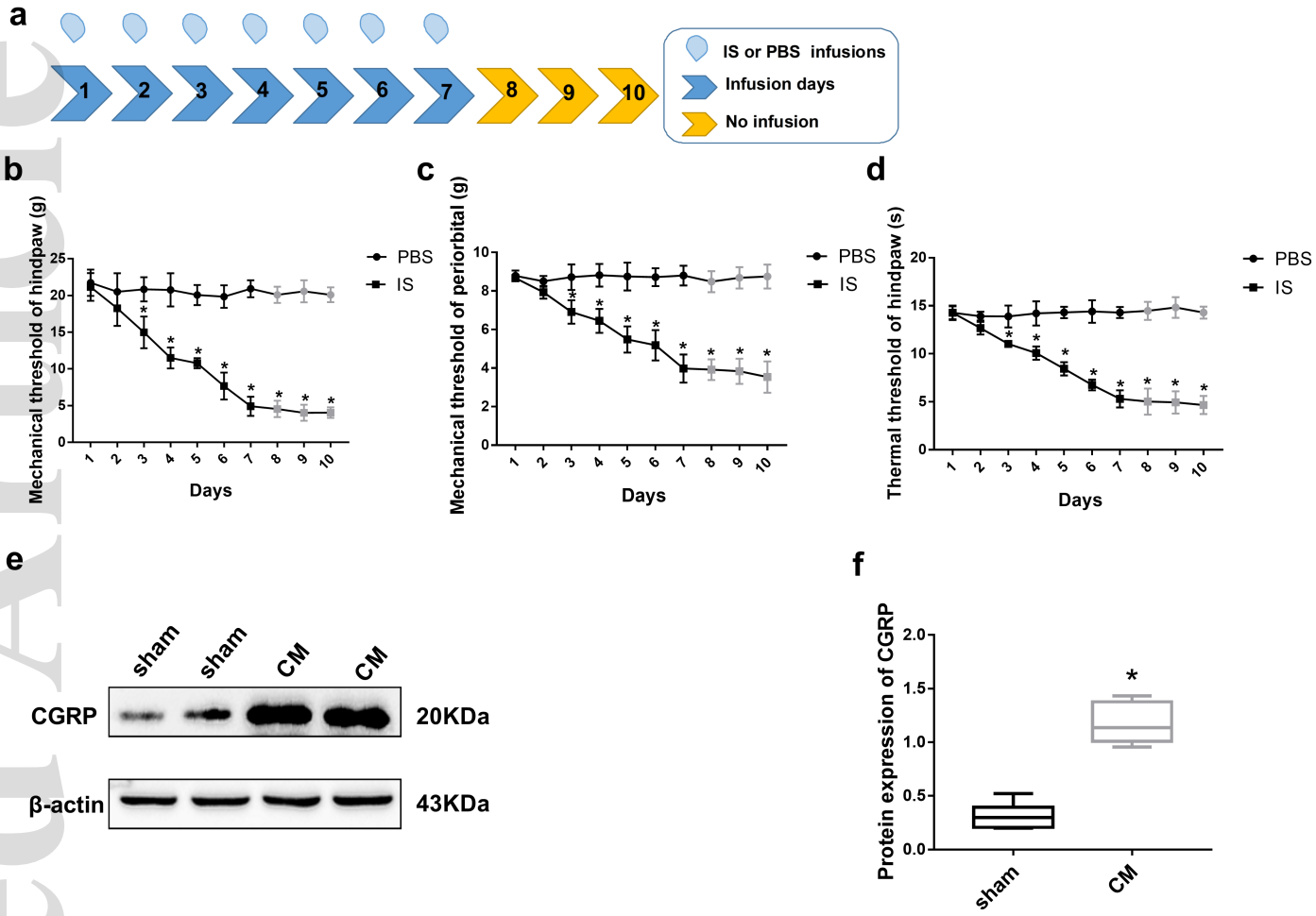

jnc_14944_f3.tif

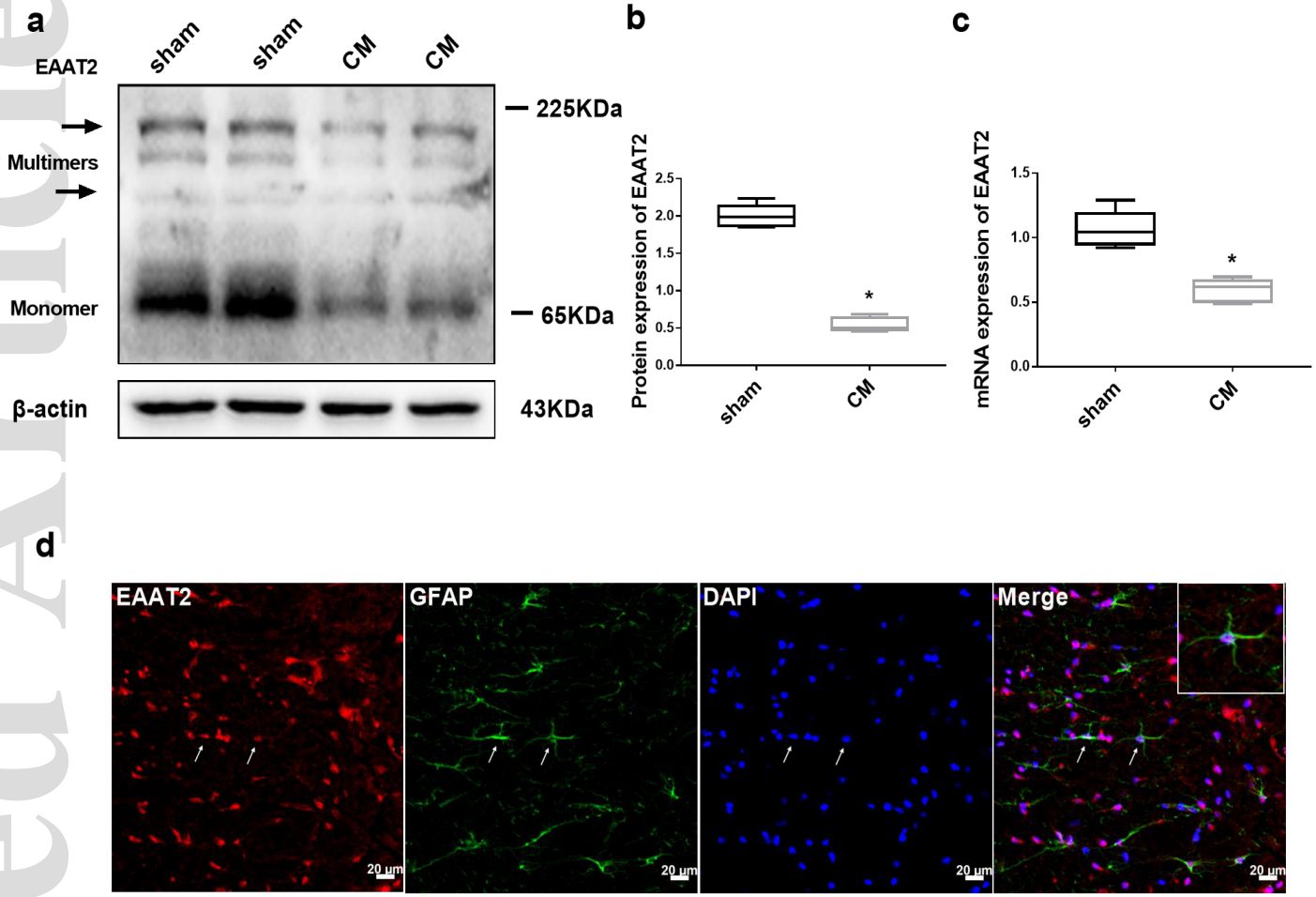

jnc_14944_f4.tif

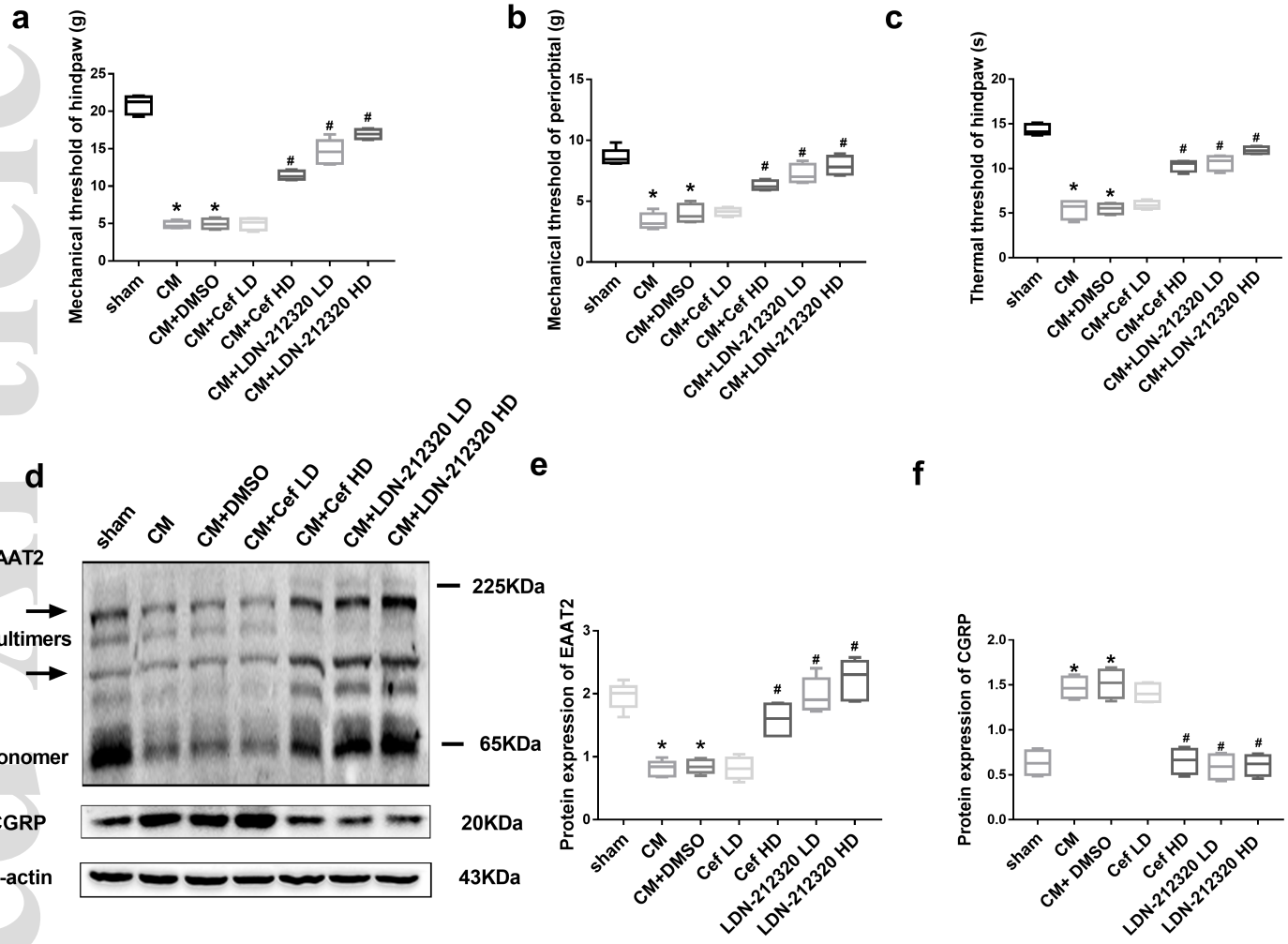

jnc_14944_f5.tif

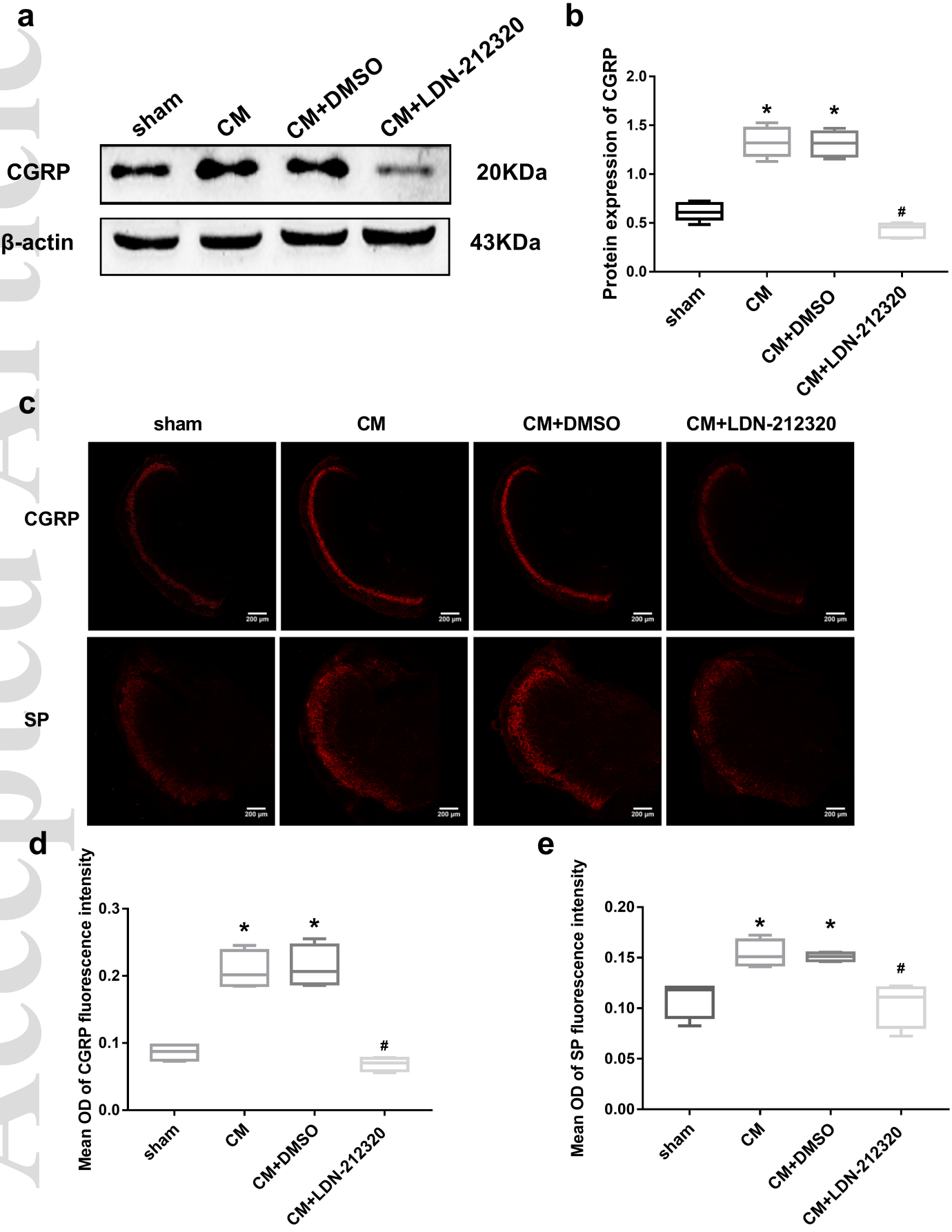

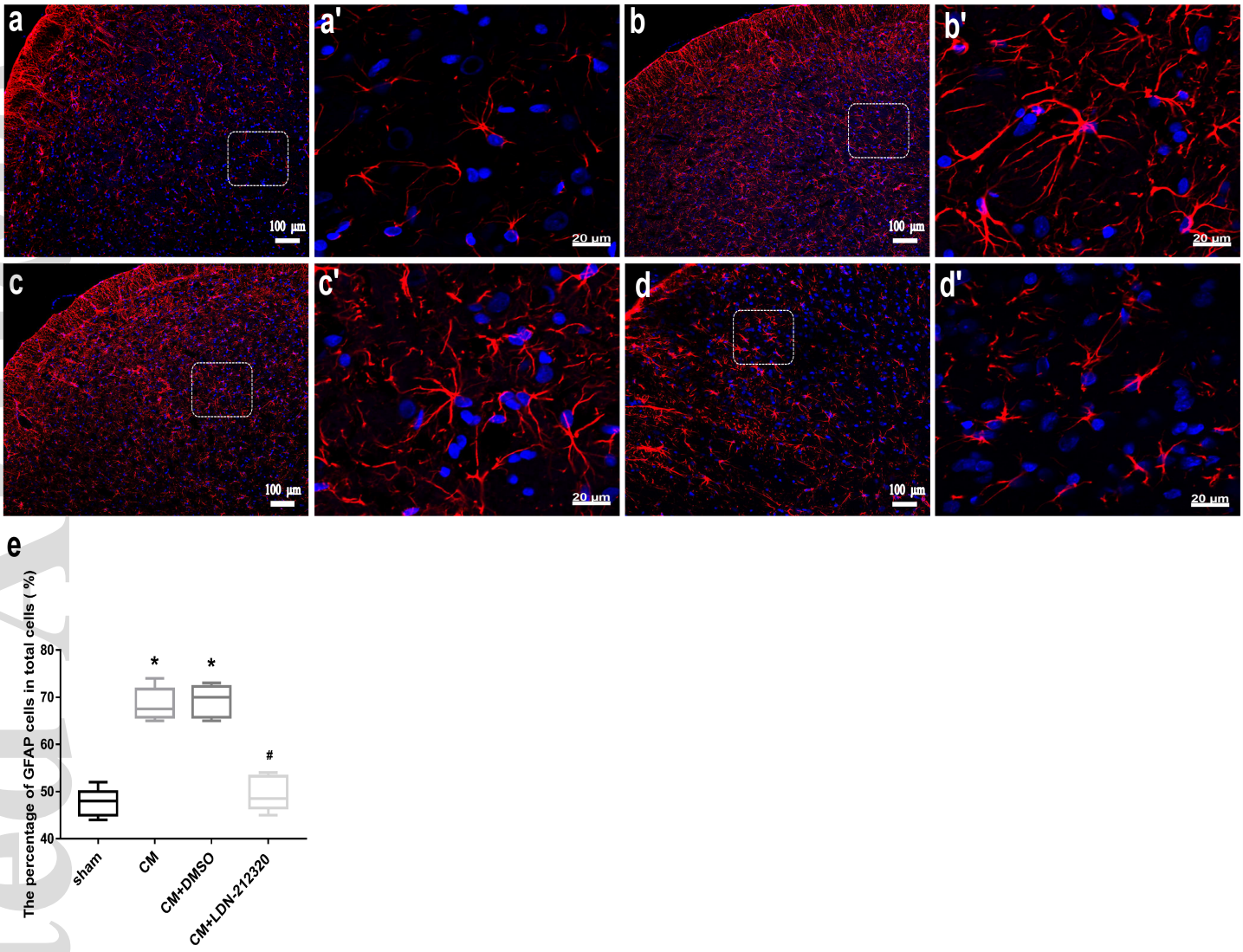

jnc_14944_f7.tif

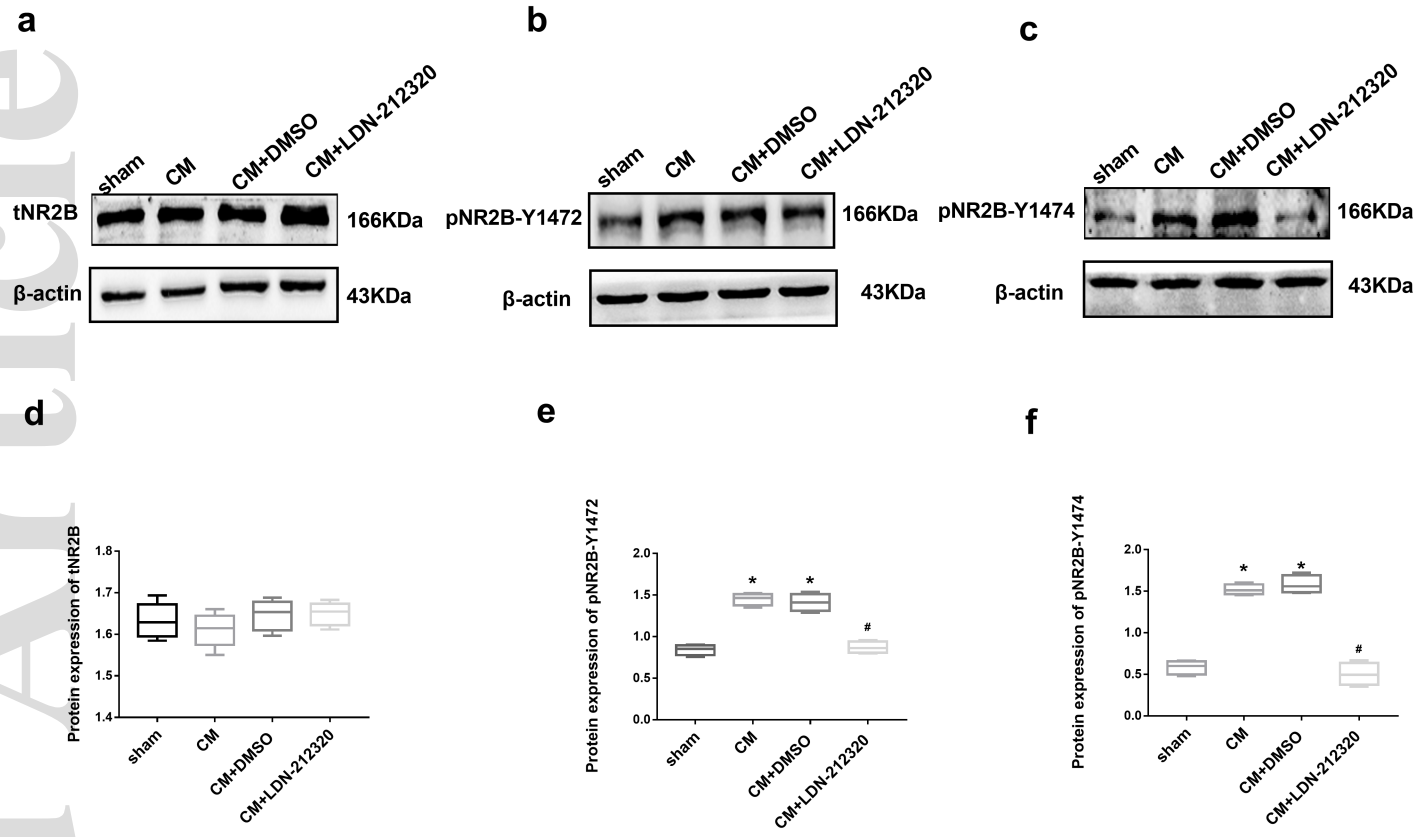

jnc_14944_f8.tif

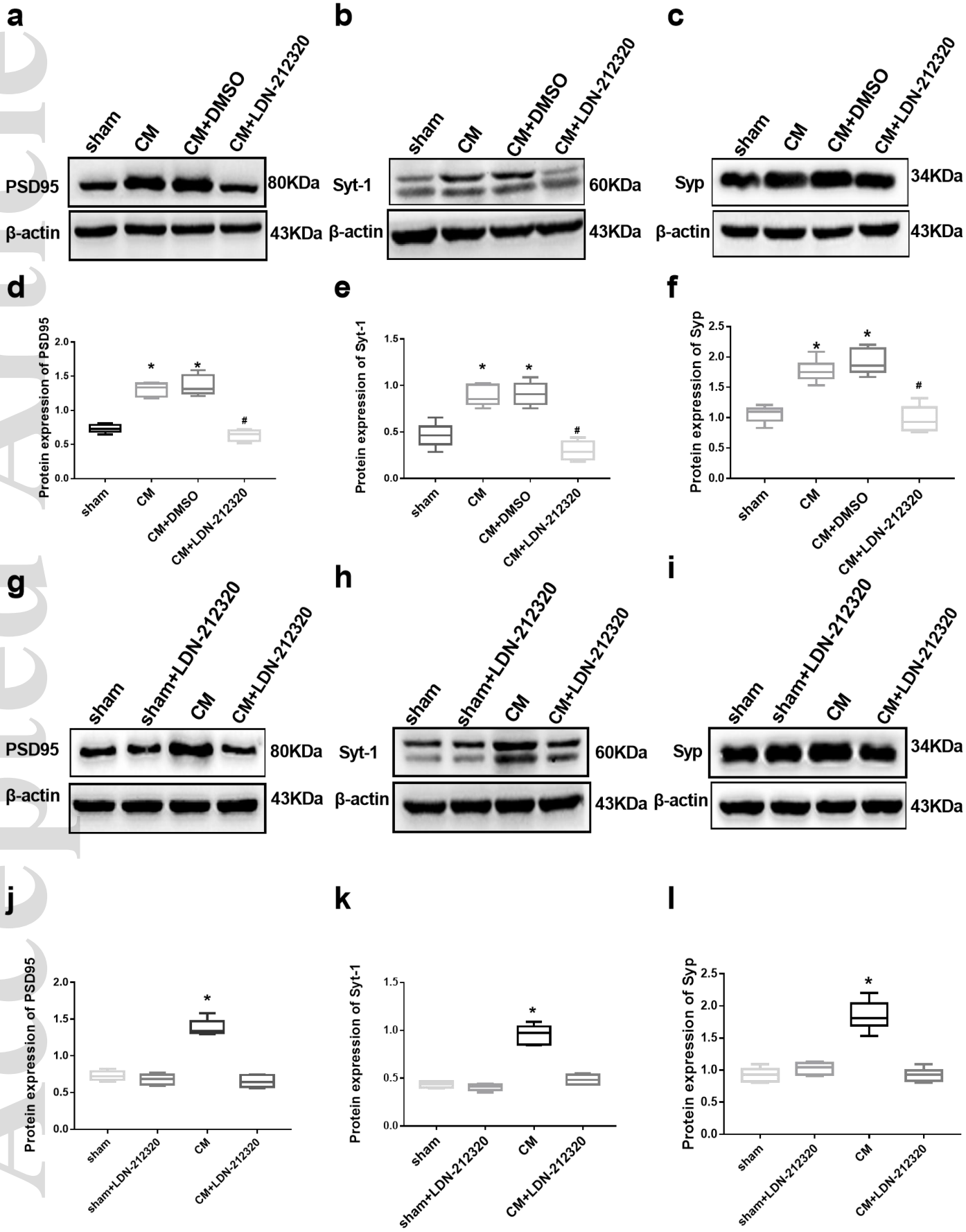

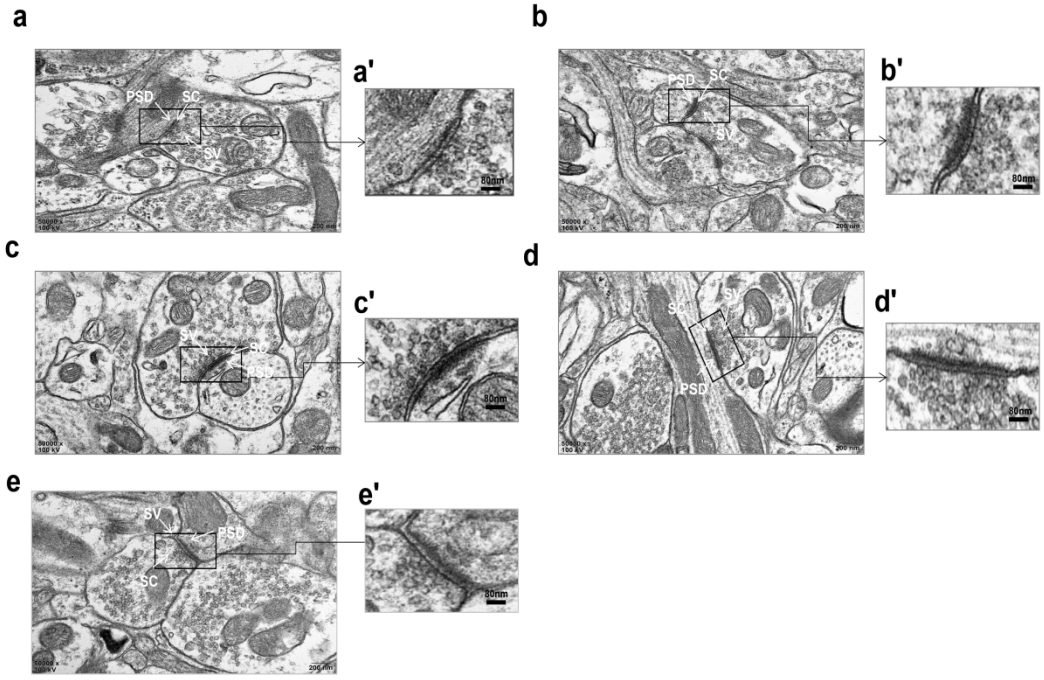

jnc_14944_f10.tif

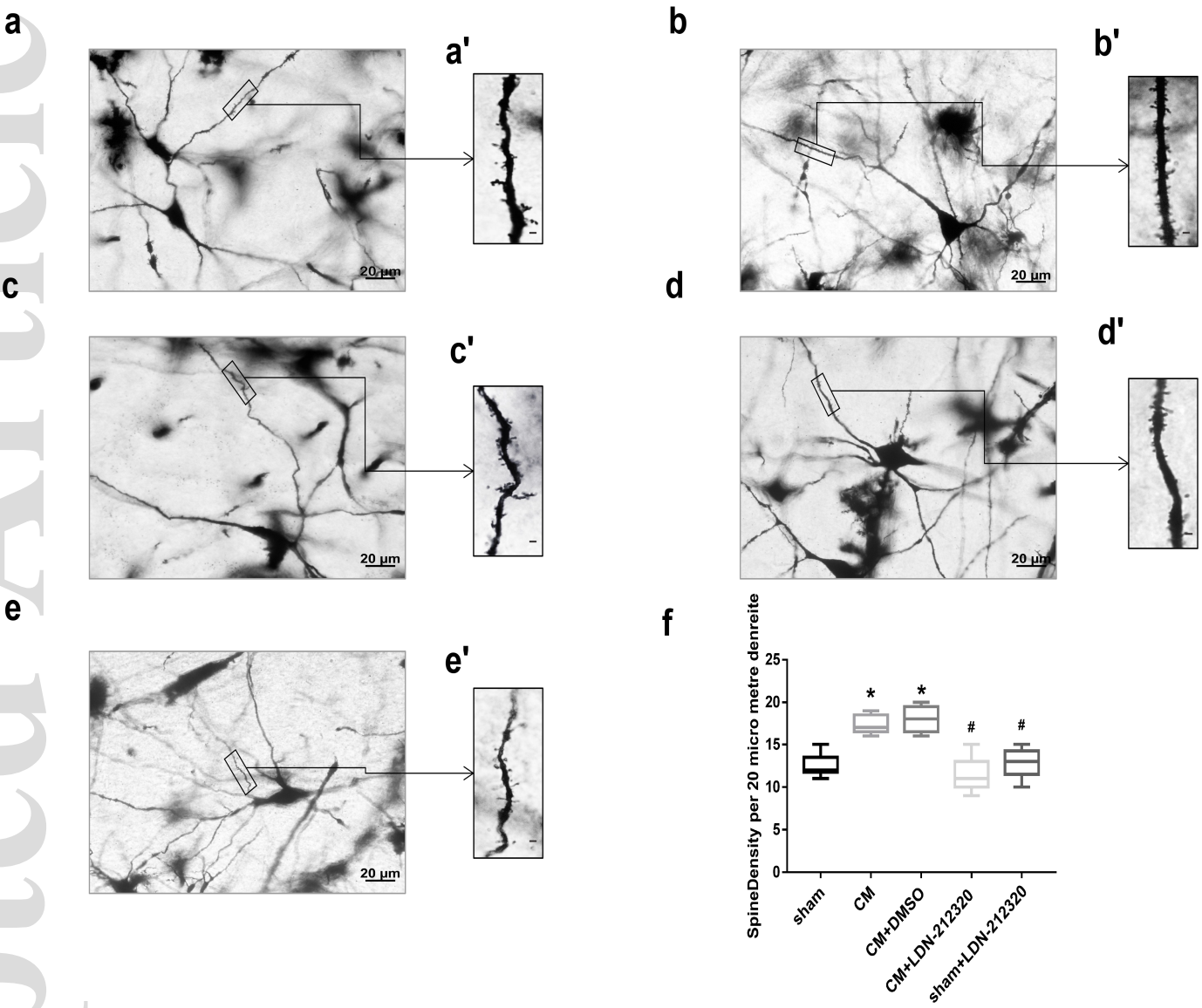

jnc_14944_f11.tif

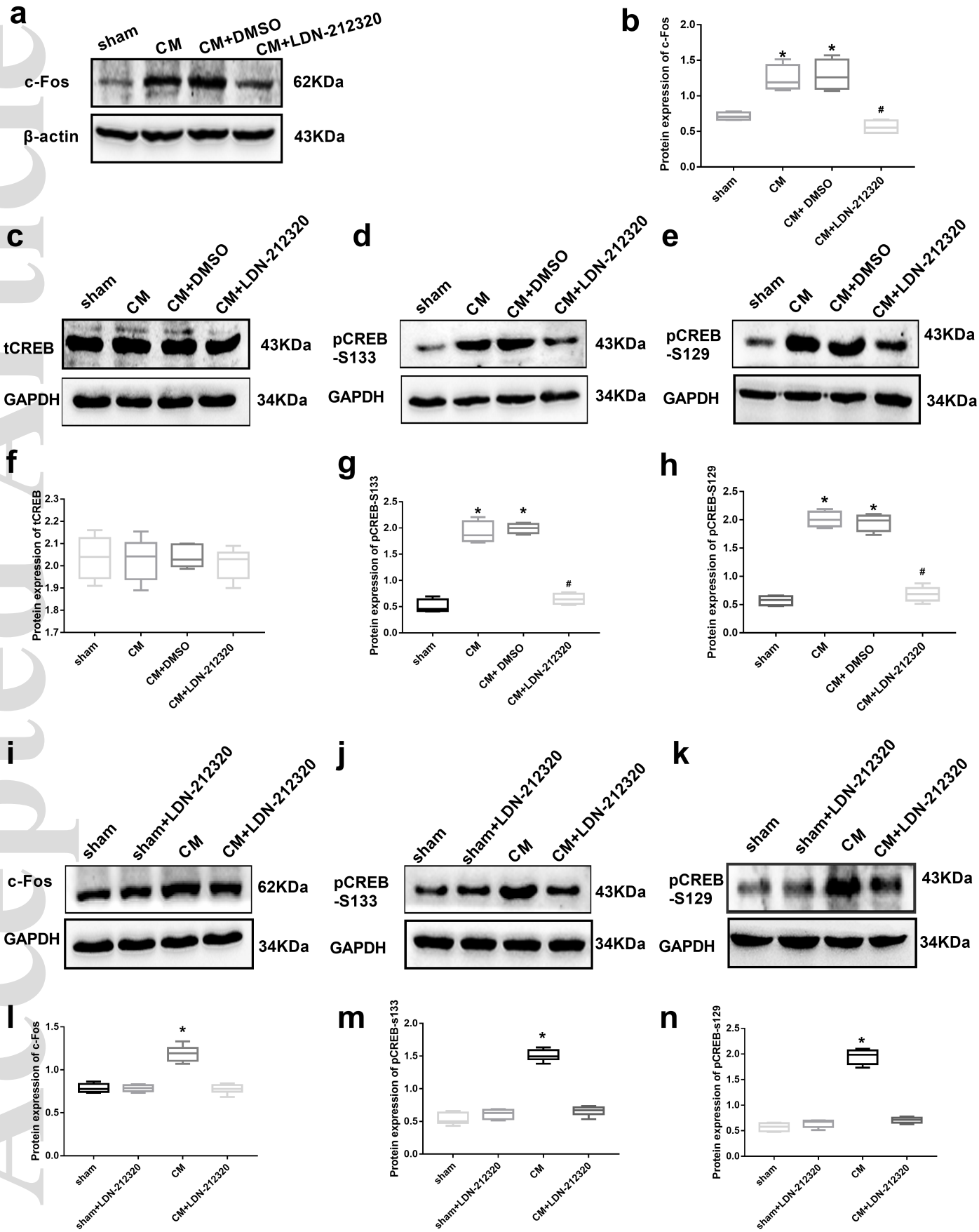

jnc_14944_f12.tif

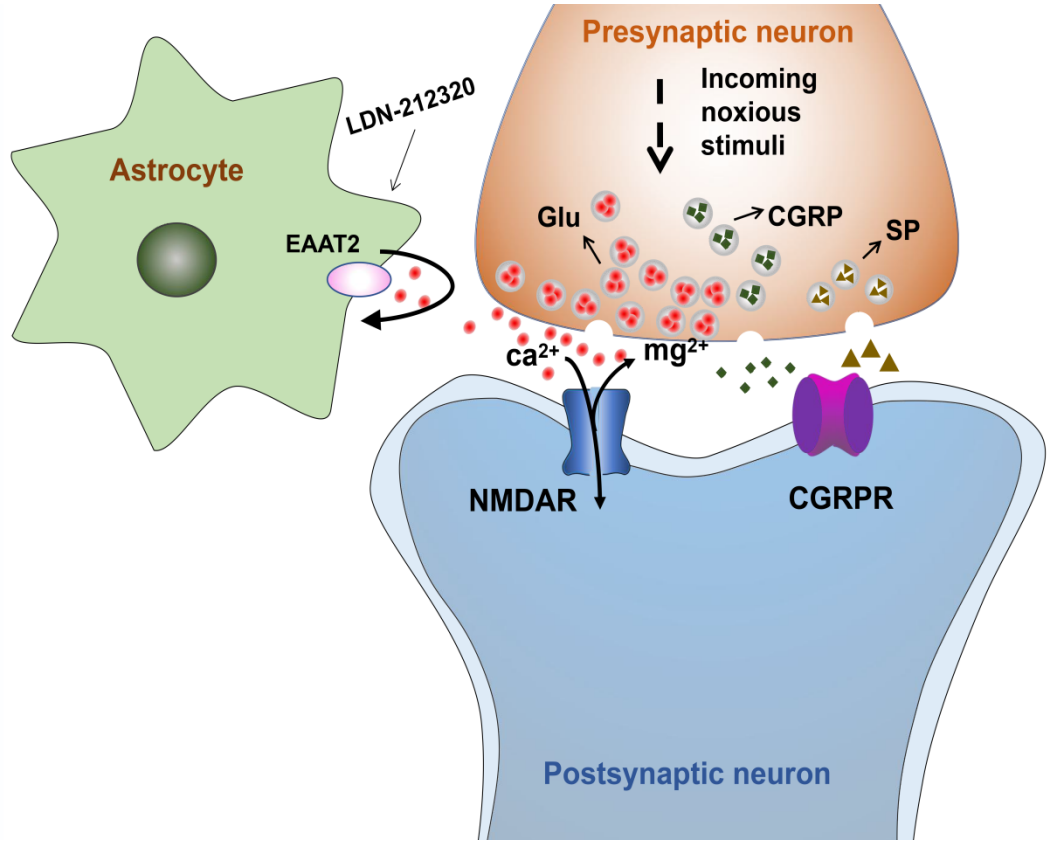

jnc_14944_f13.tif